Title page.

The genomic basis of domestic colonisation and dispersal in Chagas disease vectors.

Luis E Hernandez-Castro*[1], Anita G Villacís[2], Arne Jacobs[3], Bachar Cheaib[1], Casey C Day[4], Sofía Ocaña-Mayorga[2], Cesar A Yumiseva[2], Antonella Bacigalupo[1] Björn Andersson[5], Louise Matthews[1], Erin L Landguth[4,6], Jaime A Costales[2], Martin S Llewellyn[¶*1], Mario J Grijalva[¶2,7]

1. Institute of Biodiversity, Animal Health and Comparative Medicine, University of Glasgow, Glasgow, United Kingdom.

2. Centro de Investigación para la Salud en América Latina, Facultad de Ciencias Exactas y Naturales, Pontificia Universidad Católica del Ecuador, Quito, Ecuador.

3. Department of Natural Resources, Cornell University, Ithaca, United States of America.

4. Computational Ecology Lab, School of Public and Community Health Sciences, University of Montana, Missoula, United States of America.

5. Department of Cell and Molecular Biology, Karolinska Institutet, Stockholm, Sweden.

6. Center for Population Health Research, School of Public and Community Health Sciences, University of Montana, Missoula, United States of America.

7. Infectious and Tropical Disease Institute, Department of Biomedical Sciences, Heritage College of Osteopathic Medicine, Ohio University, Ohio, United States of America.

* Corresponding authors

Luis E Hernandez Castro: enriqhernandez18@gmail.com

Martin Llewellyn: martin.llewellyn@glasgow.ac.uk

¶ These authors contributed equally to this work.

Abstract.

The biology of vector adaptation to the human habitat remains poorly understood for many arthropod-borne diseases but underpins effective and sustainable disease control. We adopted a landscape genomics approach to investigate gene flow, signatures of local adaptation, and drivers of population structure among multiple linked wild and domestic population pairs in *Rhodnius ecuadoriensis*, an important vector of Chagas Disease. Evidence of high triatomine gene flow (F_{ST}) between wild and domestic ecotopes at sites throughout the study area indicate insecticide-based control will be hindered by constant re-infestation of houses. Genome scans revealed genetic loci with strong signal of local adaptation to the domestic setting, which we mapped to annotated regions in the *Rhodnius prolixus* genome. Our landscape genomic mixed effects models showed *Rhodnius ecuadoriensis* population structure and connectivity is driven by landscape elevation at a regional scale. Our ecologically- and spatially-explicit vector dispersal model enables targeted vector control and recommends spatially discrete, periodic interventions to local authorities as more efficacious than current, haphazard approaches. In tandem, evidence for parallel genomic adaptation to colonisation of the domestic environment at multiple sites

sheds new light on the evolutionary basis of adaptation to the human host in arthropod vectors.

Main.

The process by which insect vectors of human diseases adapt to survive and breed in human habitats is fundamental to the emergence and spread of vector-bone disease (e.g., *Aedes aegypti*[1]). Relatively modest changes in vector host preference between ancestral (wild) and derived (domesticated) forms can drive devastating epidemics that result in millions of deaths[2]. Understanding the evolution and genetic bases of traits associated with domestication in disease vectors is, therefore, paramount and could inform control efforts and reveal the epidemic potential for new vector species[3,4]. Furthermore, an accurate definition of landscape functional connectivity (the level at which the landscape heterogeneity facilitates or impedes an organism's movement from, and to, different habitat patches[5]) can shed light on the drivers of vector dispersal, and even assist in identifying poorly connected or isolated areas that can be easily targeted by eradication interventions[6–8].

Triatominae (Hemiptera: Reduviidae) are a group of hematophagous arthropods that transmit *Trypanosoma cruzi*, the parasite that causes Chagas disease, a fatal parasitic infection afflicting > 7 million people in Latin America[9]. Eradication of 'domesticated' triatomines has been the mainstay of disease control in the past (e.g., *Triatoma infestans*[10], *Rhodnius prolixus* and *Triatoma dimidiata*[11]). However, wild (e.g., *T. infestans*[12] and *R.*

prolixus[13]) and/or secondary competent species of triatomines (e.g., *Triatoma sordida*[14], *Triatoma maculata* and *Rhodnius pallescens*[15], *Panstrongylus howardi*[16] and *P. chinai*[17]) can occupy empty domestic niches and continue to jeopardise Chagas disease control strategies.

Colonisation of the domestic niche may involve multiple, independent evolutionary processes across the geographic distribution of a given vector species[18,19], analogous to parallel trophic speciation observed in other arthropods[20]. Alternately, domestication of zoonotic parasites and their vectors may result from a single or limited number of independent colonisation events, followed by rapid and widespread dispersal within the domestic setting[21,22]. Domestication of a given species may also represent a combination of these two scenarios, where multiple domesticated lineages serially introgress with wild lineages over evolutionary time, as has been elegantly demonstrated through analysis of the genomes of the domestic pig[23]. Disentangling these different scenarios in triatomine species, and their important implications for disease control, has been challenging due to a lack of genomic resources for these organisms which are only recently becoming available[24–26]. With adequate genomic tools; however, the occurrence of domestic colonisation can be established, and its underlying mechanisms unveiled. Parallel colonisation events explored using models of 'adaptation with gene flow' (e.g., [27]) can exploit standard population genetic metrics and theory to make generalisations about the genomic basis of adaptations (e.g., [20]) and reveal fundamental traits associated with the domestic niche.

Rhodnius ecuadoriensis is the major vector for Chagas disease in Ecuador and Northern Peru[28]. Both domestic and wild populations of this species exist throughout its range[29]. Preliminary morphological and genetic evidence suggests some gene flow of *R. ecuadoriensis* between domestic and wild ecotopes[30,31]. By comparison, genetic studies of *T. cruzi* infecting the same vectors in Ecuador have shown strong to moderate differentiation between wild and domestic isolates[32,33]. As such there is a lack of a clear understanding of the micro and macro-evolutionary and ecological forces shaping vector domestic adaptation and dispersal capabilities, and those of the parasites they transmit. Morphometric studies have attempted to develop phenotypic markers in triatomines associated with domestic or wild ecotopes with little (e.g. [34]) to moderate (e.g., [35]) success. Therefore, domestication in triatomines has become a rather qualitative concept[36] with urgent need for quantitative foundations.

Our study represents a first attempt to accurately quantify genomic signatures of domestication of triatomine species, as well as landscape drivers of vector dispersal. We use a reduced-representation sequencing approach (2b- RADseq) to recover genome-wide SNP variation in 272 *Rhodnius ecuadoriensis* individuals collected across ecological gradients in Loja, Ecuador. We find strong evidence of gene flow between domestic and wild ecotopes and signatures of local adaptation in some genomic regions. Furthermore, we provide substantial evidence that triatomine dispersal is fundamentally restricted by landscape elevation. Our findings suggest frequent and spatially targeted interventions, to cope with high gene flow and fragmented populations, are necessary to suppress Chagas Disease

transmission in Loja. Moreover, discovery of signatures of local adaptation shed the first light on the genomics basis of domestication in triatomines.

Results.

Recovery of SNP markers from 272 *Rhodnius ecuadoriensis* SNP specimens. Our CspCI-based 2b-RAD protocol was successful in obtaining genome-wide SNP information for *R. ecuadoriensis.* Sequencing of non-target species was minimal (0.2%) (Supplementary Figure 1). We genotyped six *Rhodnius prolixus* as controls and 80% of reads mapped to the *R. prolixus* reference genome. Only 9.5% of *R. ecuadoriensis* reads mapped to the same reference, a consequence of genomic sequence divergence between *R. ecuadoriensis* and *R. prolixus* [37]. A stringent genotyping approach confidently identified 2,552 SNP markers across 272 *R. ecuadoriensis* samples from 25 collection sites, which represented closely administrative boundaries of human communities. (Supplementary Table 1). In seven collection sites (Figure 1a; CG, BR, CE, CQ, HY, SJ and GL- seven pairs) triatomines from both domestic and wild ecotopes were collected. Remaining sites only had individuals of one ecotope (domestic or wild).

Reduced *R. ecuadoriensis* population genetic diversity in domestic ecotopes. Multiple genetic diversity estimates among populations from the 25 collection sites in Loja province were calculated (Obsvered (H_O), and expected (H_E) heterozygosity, inbreeding coefficient (F_{IS}) and Allelic Richness (A_r); Supplementary Table 2). Sample-size corrected A_r values ranged from 1.19 to 1.44 with the lowest values in La Extensa (EX), San Jacinto (SJ), El

Huayco (HY) and Santa Rita (RT). In the paired ecotopes within the seven collection sites, A_r values were higher for wild than domestic triatomine populations in five out of seven instances, a significant effect observed ($p<0.05$, rarefaction method[38]).

Genomic differentiation between domestic and wild ecotopes. To assay populations dynamics between sympatric domestic and wild foci, we focused our individual-based genomic differentiation and pairwise F_{ST} comparisons analyses on the seven collection sites for which samples from both ecotopes were available (Figure 1a). Supporting frequent migration between domestic and wild ecotopes, samples from each ecotope were interleaved at most collection sites in the phylogenetic tree, with collection site geography, not ecotope, impacting the tree topology (Figure 1b). As such, samples collected in Galapagos (GL), Coamine (CE) and Chaquizhca (CQ) formed distinct clusters, and El Huayco (HY) - San Jacinto (SJ) and Bramaderos (BR) - La Cienega (CG) also grouped discretely. Five broadly congruent clusters were defined in a discriminant analysis of principal components (DAPC) (Figure 1c), with geographic collection site rather than their ecotope again structuring observed diversity. F_{ST} indices between paired domestic and wild triatomine samples within each of the seven compared collection sites indicate little differentiation (e.g., $F_{ST} \leq 0.10$). Permutation tests indicated that F_{ST} was significant ($p < 0.05$) at only two sites - Bramaderos and El Huayco (Figure 1d). As expected, hierarchical analysis of molecular variance revealed genetic subdivision was significantly stronger ($F_{\text{collection sites/total}} = 0.26$, p-value < 0.001) among collection sites than among ecotopes within collection sites ($F_{\text{ecotope/collection site}} = - 0.004$, p-value < 0.001) or among collection year within communities ($F_{\text{collection year/collection site}} = 0.06$, p-value < 0.001) (Supplementary Table 4).

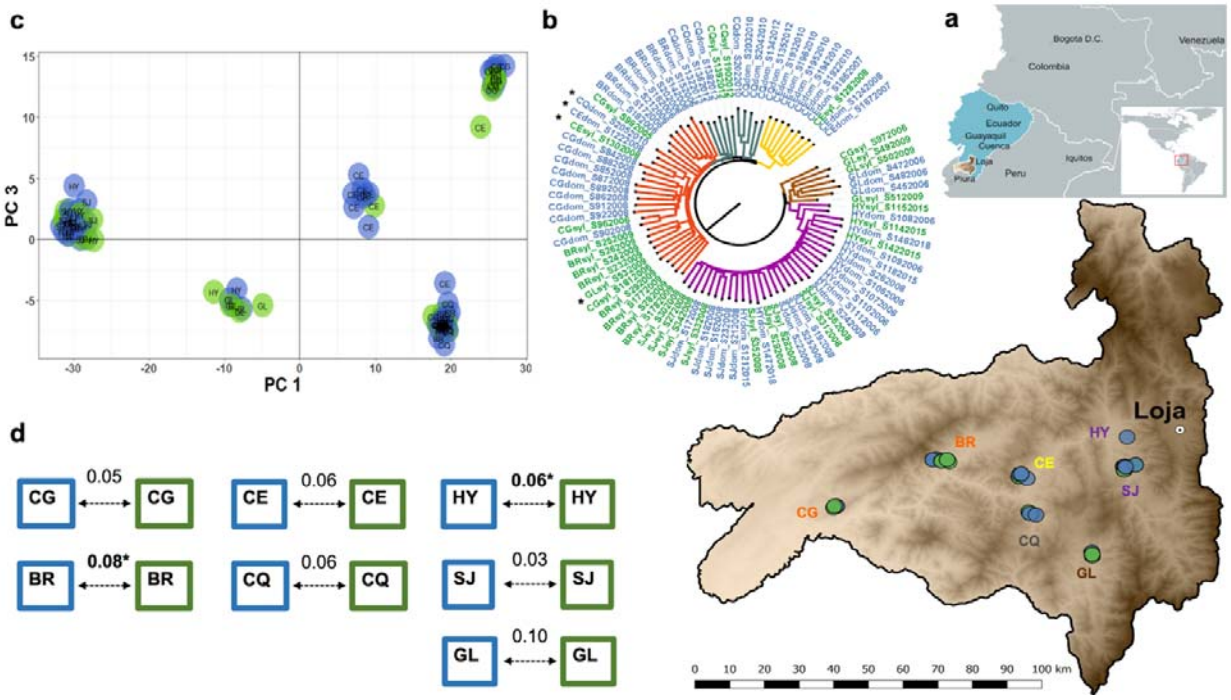

Figure 1. Genomic differentiation of domestic and wild *R. ecuadoriensis.* a, geographic distribution of the seven collection sites with both ecotopes over an elevation surface map of Loja. **b**, Neighbor-Joining midpoint phylogenetic tree with phylogenies indicating the Euclidean distance between triatomine samples built from allele counts. Tree branches clades are colour-coded to approximately differentiate collection sites (or clusters of collection sites) with few samples (black asterisks) not conforming to the pattern. **c**, the scatter plot shows five clusters are built with the first and third principal components of the discriminant analysis eigenvalues. **d**, pairwise F_{ST} comparisons between domestic (blue box) and wild (green box) *R. ecuadoriensis* in multiple sites across Loja (**a**). Significant F_{ST} values (arrows) after FDR correction are highlighted in bold and an asterisk. In all panels, samples location (dots) and labels are colour-coded to indicate their domestic (blue) or wild (green) collection ecotope. Collection sites 2-letter ID labels: SJ, San Jacinto; HY, EL Huayco; GL, Galapagos; CQ, Chaquizhca; CE, Coamine; BR, Bramaderos; CG, La Cienega (see Supplementary Table 1 for full collection sites list).

177 **Genetic loci correlated with domestic colonisation.** To identify loci associated with
178 domestic colonisation, we combined a Random Forest (RF) classification approach and
179 redundancy analyses (RDA) with outlier scans. We included the seven collection sites with
180 frequent domestic-wild migration and three additional wild-only sites to roughly conform
181 similar number of domestic (n= 56) and wild (n= 52) samples. A total of 347 SNPs provided
182 high ranked classification accuracy (mean > 3) across the three RF iterations (inset in Figure
183 2a). Backwards purging on this highly discriminatory subset of SNPs detected a set of 43
184 SNPs that minimised the 'Out-of-bag' error rate (OOB-ER) to a minimum of 0.09 and
185 maximised the discriminatory power among domestic and wild samples (Figure 2a). In a
186 parallel RDA model, ecotope (domestic / wild) was a predictor explaining approximately
187 0.4% of the total variation and the constrained axis built from that variation was significant
188 (p-value < 0.001), and so was the full model as indicated by the Monte Carlo permutation
189 test. The distribution of each SNP loading/contribution to the RDA significant axis showed
190 109 candidate adaptive loci as SNPs loadings at ±2 SD from the mean of this distribution
191 (permissive threshold; Figure 2b). In a more conservative approach, we also identified seven
192 loci from those 109 under very strong selection as represented by those SNPs loading at the
193 extreme ±3 SD (conservative threshold) away from the mean distribution of the constrained
194 axis (Figure 2b). The arrangement of the individual samples in the ordination space with
195 relation to the RDA axis showed a clear pattern of subdivision comparable to the ecotope in
196 which samples were collected (Figure 2c). The 21 loci/SNPs identified as adaptive loci (dark
197 dots in Figure 2b) by RDA were also detected as highly discriminatory SNPs for domestic
198 and wild ecotopes in the RF analysis. Assuming 'adaptation with geneflow' we assessed
199 locus-specific estimates of F_{ST} (Figure 2d), among the 2552 SNPs between domestic and

wild ecotopes and identified one SNP (Locus ID 15732 – purple diamond in Figure 2bd) likely to be under local adaptation and/or spatial heterogeneous selection as suggested by OutFlank analysis (Figure 2d left). Moreover, outlier scan with fsthet (Figure 2d right) in the same subset flagged this OutFlank SNP and 73 additional SNPs showing F_{ST} higher that the average neutral loci distribution at a 5% threshold. In summary, 43 SNPs were identified with the highest classification accuracy in RF analysis. 21 of those SNPs showed some signal of adaptation (that is, loaded ± 2 SD away from mean distribution of contrained axis) and 4 were identified showing strong signal of adaptation (that is, loaded ± 3 SD away from mean distribution of contrained axis) in RDA analysis. Three of the SNPs flagged as outliers in fsthet analysis were found also being at high classification accuracy in RF analysis. The SNP (Locus ID 15732) likely to be under strong selection as identified by OutFlank analysis, also had a high classification accuracy in RF and, interestingly, it was also identified within the RDA and fsthet SNPs sets under strong signal of selection.

Mapping outlier loci to the *Rhodnius prolixus* genome. Several SNPs from the different analyses mapped to annotated regions of the *R. prolixus* genome. One SNP identified in the RDA analysis mapped (97.1% identity) in a *R. prolixus* genome region containing the characterised *Krüppel* gap gene (Accession No JN092576.1) involved in embryo development in arthropods[39]. Three SNPs likely to be under balancing selection identified in fsthet analysis mapped (100% identity) to regions in the *R. prolixus* genome containing characterised GE-rich and polylysine protein precursors (mRNA - Accession AY340265.1), and the *Krüppel* and giant gap genes[39,40] (Accession No HQ853222.1). The former are important proteins within the sialome of blood-sucking bugs[41] and the latter involved in

223 embryo development[40]. Mapping of the majority of putatively adaptive SNPs, including Locus
224 ID 15732, was not possible in the absence of an available *R. ecuadoriensis* genome.
225

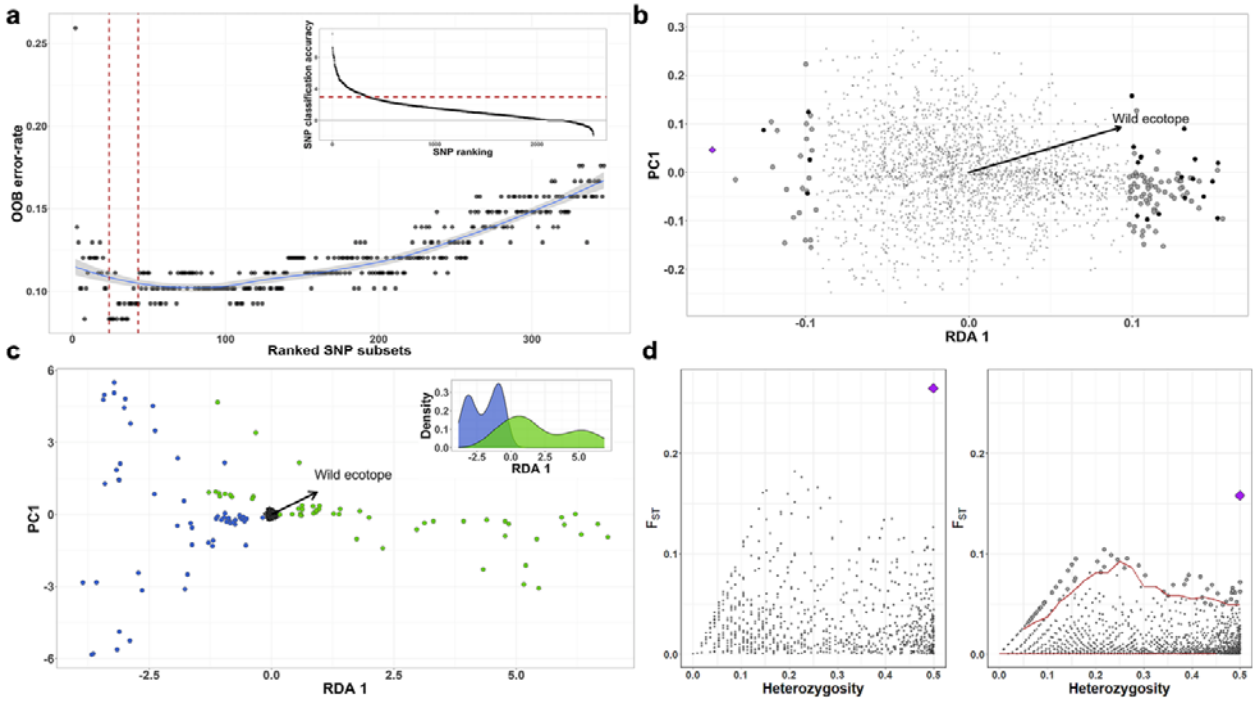

226

227 **Figure 2. Scanning outlier SNP markers for signatures of local adaptation. a**, Random Forest
228 backwards purging shows subsets with decreasing number of highly discriminatory SNPs and their
229 resulting OOB-ER. The two vertical red lines indicated the 43 SNPs subset with the lowest OOB-ER
230 and maximum discriminatory power between domestic and wild ecotopes. The inset shows SNPs
231 ranked based on their classification accuracy averaged after 3-independent RF runs. SNPs with
232 classification accuracy above three (red horizontal line) were used for the backwards purging. **b**, In
233 our RDA model, SNPs (dots and diamonds) are arranged as a function of their relationship with the
234 constrained predictor, ecotope (arrow outlines towards a wild ecotope relationship). SNPs closer to
235 the centre (small grey dots) are not showing relation with the predictor. Adaptive loci/SNPs are
236 represented by those large dots/diamond loading at ± 2 SD and ± 3 SD separated from the mean
237 SNPs loading distribution. Black large dots (and purple diamond) represent loci/SNP identified with
238 high classification power in RF analysis. **c**, a biplot of *R. ecuadoriensis* triatomine smaples and SNPs
239 (small black dots in the centre) are arranged in relation to the constrained RDA axis with an arrow
240 indicating those related to the wild ecotope. Dots are colour-coded to show sample ecotope of
241 collection, domestic (blue) or wild (green). Biplot scaling is symmetrical with inset showing the density
242 function for the RDA axis. **d**, Scatter plots show OutFlank (left) and fsthet (right) SNPs F_{ST}-

heterozygosity relationship. 43 SNPs (large dots) had higher than average F_{ST} distribution of neutral loci in fsthet, whereas only one in OutFlank. Purple diamond indicated the SNP (ID 15732) flagged in all four analyses.

Comparison of dispersal rates of *R. ecuadoriensis* between domestic sites with dispersal rates between wild sites. Including all samples (n = 272) and collection sites (n = 25), we tested the strength of genetic isolation-by-distance (IBD) initially among domestic sample collection sites and latterly among wild collection sites (Figure 3). Mantel tests in both domestic (r_m = 0.46, p-value < 0.001) and wild (r_m = 0.31, p-value = 0.043) ecotopes strongly supported an effect of geographic distance on genetic distance (Figure 3a). Based on a generalised least square model (Supplementary Table 5) with maximum likelihood population effects parametrisation (GLS-MLPE), the effect of geographic distance significantly stronger (0.0018, p-value < 0.001) in wild compared to domestic foci (Figure 3a), suggesting that the rate of vector dispersal occurred at a higher rate between domestic populations than between wild ones.

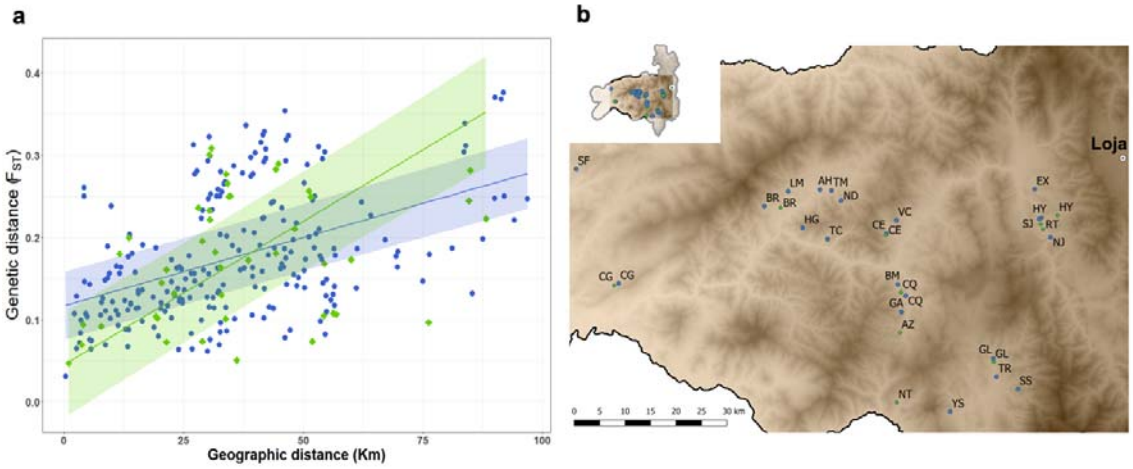

Figure 3. Dispersal rate in *R. ecuadoriensis*. a, correlation between pairwise genetic (F_{ST}) and geographic distances (data points) with fitted regression lines (95% CI) for domestic (blue dots) and wild (green diamonds) ecotopes. Fitted GLS-MLPE model in eqn 1. **b**, geographic distribution of the 25 collection sites across Loja province used for estimating *R. ecuadoriensis* gene flow with geographic distance. Collection sites 2-letter ID labels: EX, La Extensa; SJ, San Jacinto; HY, EL Huayco; RT, Santa Rita; NJ, Naranjillo; GL, Galapagos; SS, Santa Rosa; TR, Tuburo; YS, Camayos; NT, San Antonio de Taparuca; AZ, Ardanza; GA, Guara; CQ, Chaquizhca; BM, Bella Maria; CE, Coamine; VC, Vega del Carmen; TM, Tamarindo; HG, Higida; ND, Naranjo Dulce; TC, Tacoranga; AH, Ashimingo; LM, Limones; BR, Bramaderos; CG, La Cienega; SF, San Francisco (SF).

Landscape functional connectivity in *R. ecuadoriensis*. Landscape genomic mixed modellling aims to identify the effect of different combinations of landscape surfaces and their parameters on a given genomic differentiation pattern. To obtain an accurate representation of the genomic differentiation pattern among *R. ecuadoriensis* populations, we chose Hedrick's G_{ST} pairwise comparisons (Figure 4b) which corrects for sampling limited number of populations[42]. The genomic pattern was consistent regardless of metric used (e.g., Pairwise F_{ST} [43] and Meirman's standardised F_{ST} [44]) as revealed by strong and significant ($r^2 = 0.99$ & 0.92, respectively; $p < 0.001$) Pearson's correlations. Pairwise Hedrick's G_{ST} comparisons showed a strong pattern of population structure across Loja province with presence of both high and low genetic differentiation among collection sites (Figure 4ab). San Francisco (SF) and San Antonio (NT) were two examples of clear, and mutually distinct, outliers in genetic terms. Santa Rita (RT), El Huayco (HY), San Jacinto (SJ) and La Extensa (EX) were genetically and geographically close but highly differentiated form the rest. Overall, clusters of collection sites were evident with some differentiation within and among clusters (Figure 4b).

The genomic pattern was iteratively regressed with different combinations of landscape variables and parameters using the ResistanceGA[45] optimisation framework (see Methods). The optimisation process involves estimating unbiased resistance values for a given combination of surfaces and select the best (true) model representing the genomic pattern. To rule out collinearity between landscape variables, we calculated Spearman's correlation coefficient, rho, between all pairs of surfaces which resulted in small and/or negative (rho < 0.29) correlations (Supplementary Table 8). Similarly, a scatterplot matrix did not show highly correlated surfaces (Supplementary Figure 11).

Our three ResistanceGA optimisation replicates (see Methods) showed comparable results. In all replicates, the single elevation surface showed the lowest AIC_c values and the highest AIC_c weight compared to the other single and composite optimised surfaces (Table 1 is a replicate example). Delta AIC_c shows the AIC_c difference between the elevation surface (best model) and the rest of the (combination of) surfaces. A difference of ~2.26 units between elevation surface and a distance-only model was evident which suggests elevation surface is a better predictor that geographic distance. Optimisation of the elevation surface parameters confirmed gene flow resistance increases with altitude up to the highest resistance at approximately 2,400 m.a.s.l. (Supplementary Figure 12).

To evaluate the roboustness of our optimisation procedure and test the effect of uneven distribution of sample sites, we ran a bootstrap analysis with resampling of the sites at each iteration. Interestingly, the bootstrap analysis revealed that, when resampling 85% of the collection sites, the optimised elevation surface model was ranked the top model in only

310 43.2% of the bootstrap iterations compared to 46% of the times in which a distance-only
311 model was better (Table 2). The fact that elevation surface was slightly less supported in the
312 bootstrap analysis is likely due to the irregular distribution of sites across the study area and
313 altitudes. Nevertheless, elevation surface remains the strongest predictor of genetic
314 connectivity across the study area (Table 1).

315

316 **Table 1 Model selection results for the generalised mixed-effects models optimised on genetic**
317 **distance (Hedrick's G_{ST}) for *R. ecuadoriensis*.** For each resistance surface model, number of
318 parameters plus the intercept (k), Akaike information criterion (AIC), additional parameters corrected
319 AIC (AIC_c), marginal (R^2m) and conditional (R^2c) R^2 values of the fitted MLPE model, log-likelihood
320 (LL), delta AIC_c and AIC_c weight (ω) are provided.
321

Resistance surface model	Type	*k*	AIC	AIC_c	R^2m	R^2c	LL	Delta AIC_c	ω
Elevation	single	4	-751.51	-749.51	0.41	0.72	379.76	0	0.76
Distance	single	2	-743.79	-747.25	0.43	0.74	375.90	2.26	0.24
Roads	single	6	-744.91	-736.25	0.42	0.75	376.46	13.26	0.0010
Elevation + Roads	composite	9	-751.55	-729.55	0.42	0.72	379.77	19.96	3.49e-05
Land	Single	12	-762.26	-720.26	0.52	0.81	385.13	29.25	3.35e-07
Elevation + Land cover	composite	15	-763.15	-687.82	0.57	0.78	385.57	61.70	3.03e-14
Land cover + Roads	composite	17	-762.06	-648.63	0.56	0.78	385.03	100.88	9.37e-23
Null model	single	1	-561.25	-565.08	0	0.42	283.63	184.43	6.75e-41
Elevation + Land cover + Roads	composite	20	-762.44	-520.44	0.55	0.78	385.22	229.08	1.36e-50

322

323 **Table 2 Summary of bootstrap analysis.** For each resistance surface model, number of parameters
324 plus the intercept (*k*), and average (Avg) of the Akaike information criterion (AIC), additional
325 parameters corrected AIC (AIC_c), AIC_c weight (ω), rank, R^2m, LL, root mean square error (RMSE) and
326 frequency the model was top ranked are provided.
327

Resistance surface model	*k*	Avg AIC	Avg AIC_c	ω	Avg rank	Avg R^2m	Avg LL	Avg RMSE	Top model (%)
Elevation	4	-535.59	-533.09	0.40	1.62	0.41	271.79	0.055	43.2

Distance	2	-531.44	-530.78	0.60	2.33	0.42	267.72	0.055	46
Land cover	12	-526.59	-487.59	4.17e-05	3.91	0.51	275.30	0.053	10.8
Roads	6	-523.81	-517.81	0.0008	4.18	0.41	267.91	0.055	0
Elevation + Roads	9	-525.76	-509.40	2.80e-06	4.40	0.41	271.88	0.055	0
Elevation + Land cover	15	-521.94	-425.94	1.45e-21	5.29	0.55	275.97	0.054	0
Land cover + Roads	17	-516.51	-312.51	3.97e-46	6.59	0.54	275.26	0.054	0
Elevation + Land cover + Roads	20	-511.14	328.86	1.11e-185	7.68	0.54	275.57	0.054	0

To assist with the identification of vector management zones for regional health authorities, an electrical current map was built by applying a circuit theory algorithm[46,47] on the optimised elevation surface model (Figure 4c). Specifically, the algorithm simulates the passing of an electric current across grids (zones) with low/high optimised resistance values. Low resistance grids are highlighted as high current intensity zones (yellow/light zones in Figure 4c) in which high population connectivity, and therefore high degree of gene flow, is predicted. The map showed different gradients of connectivity within and among western, central, eastern and southern Loja province. These included individually isolated populations (e.g. SF & CG), isolated clusters (e.g EX; SJ; HY; RT; NJ); as well as well-connected hubs (e.g., BR-LM, AH-TM-ND, HG-TC and CE-VC).

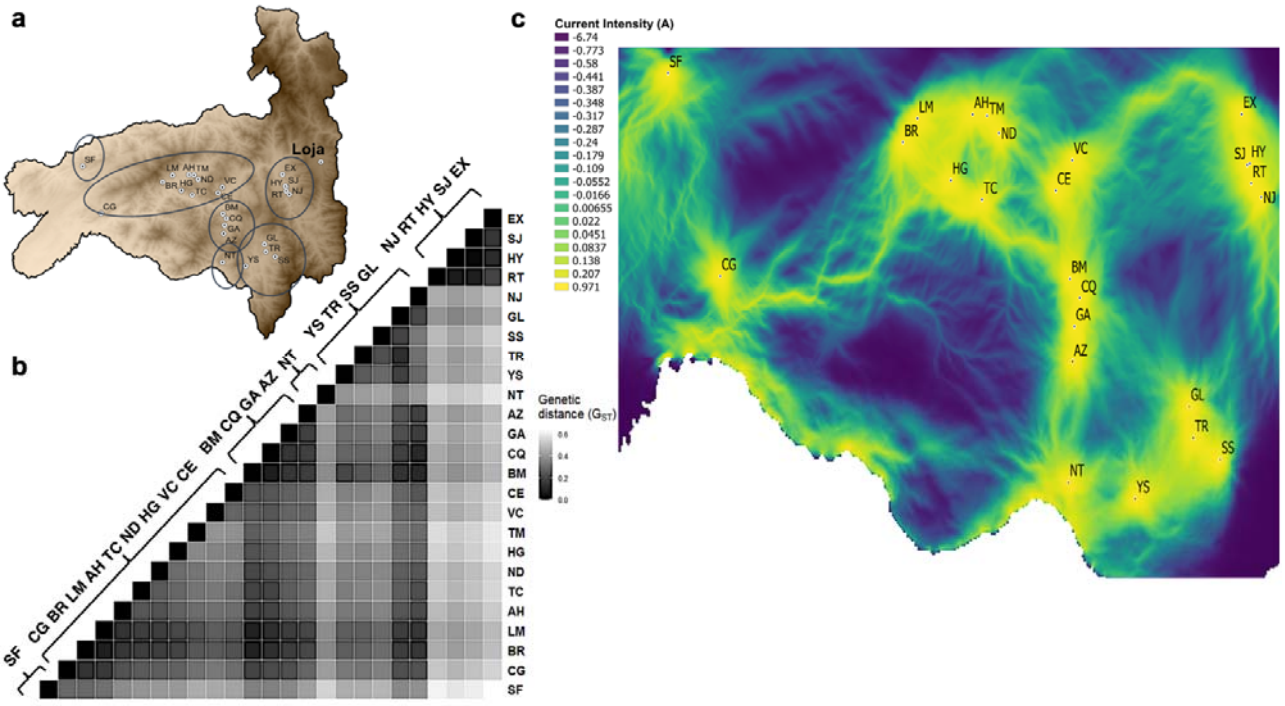

Figure 4. Landscape connectivity of *Rhodnius ecuadoriensis* in Loja province, Ecuador. a, Map of the geographic location of collection sites across Loja. **b**, Heatmap shows pairwise genetic distances (G_{ST}) with collection sites ID labels on the right. Clusters and highly differentiated collection sites are circled in **a.** Grey scale indicate genetic distance with lighter colours showing higher differentiation. **c**, Electrical current map of Loja built from the optimised elevation surface model showing a gradient of high (yellow/light shade), medium (light greens) and low (blue/dark shade) functional connectivity across Loja. Clusters of highly connected sites are evident but isolated sites are also present across regions on Loja. Connectivity within and among clusters and collection sites is highly influenced by the landscape, specifically elevation surface.

Discussion.

In this study we make several core observations: *R. ecuadoriensis* do invade houses from wild populations, genomic signatures of *R. ecuadoriensis* domestication can be functionally mapped, and the landscape drivers of vector dispersal can be identified. Consistent with frequent house invasion, high levels of gene flow between multiple domestic and wild *R. ecuadoriensis* populations were detected by hierarchical analysis. Low and largely non-significant pairwise F_{ST} values, as well as interleaved sample clustering based on phylogenetic and discriminant analyses were also consistent with house invasion. Significantly elevated allelic richness in wild sites by comparison to nearby domestic foci clearly confirmed that dispersal occurred most frequently from wild ecotopes into domestic structures. Genome scans across these parallel domestication events revealed strong evidence of 'adaptation with geneflow', with key outlier loci associated with colonisation of human-made domestic structures and, presumably, human blood feeding - several of which mapped to the *R. prolixus* genome. A strong signature of isolation-by-distance (IBD) was observable throughout the dataset, an effect less pronounced between domestic sites than between wild foci. Formal landscape genomic analyses revealed elevation surface as the major barrier to genetic connectivity between populations. Landscape genomic analysis enabled a spatial model of vector connectivity to be elaborated, informing ongoing control efforts in the region and providing a model for mapping the dispersal potential of triatomines and other disease vectors.

379 Vector control is the mainstay of Chagas Disease control[11]. Widespread wild reservoir hosts,
380 as well as a lack of safe treatment options[48,49] and associated healthcare infrastructure,
381 mean that transmission cannot be blocked by reducing parasite prevalence in human and
382 animal hosts[50]. Our data indicate that elimination of domesticated *R. ecuadoriensis* in
383 Ecuador will be frustrated by repeated re-invasion from the wild environment. Similar risks to
384 effective control are posed by wild *T. infestans* in the southern cone region[12], *R. prolixus* in
385 Los Llanos of Colombia and Venezuela[13] and potentially elsewhere in Latin America where
386 competent vectors are present in the wild environment and nearby domestic locales (e.g., *T.*
387 *sordida, T. maculata, R. pallescens* and others[14,15]).
388
389 Understanding evolutionary processes that underpin the colonisation of the domestic
390 environment by arthropod vectors, and their specialisation to feeding on humans, is required
391 to characterize their vectorial capacity. Hybrid ancestry in *Culex pipiens*, for example, is
392 thought to contribute to the biting preference for humans[51]. Human feeding preference can
393 be rapidly genetically selected for in *Anopheles gambiae*[52]. Specialisation of *Aedes aegypti*
394 on humans, and resultant global outbreaks of dengue, yellow fever, and Chikungunya
395 viruses, may be traceable to the emergence of a differential ligand-sensitivity of the odorant
396 receptor *AaegOr4* in East Africa[2]. In triatomines, the nature of genetic adaptions that have
397 enabled the widespread dispersal of successful lineages are far from clear. *T. infestans*,
398 thought to have originated in the Western Andean region of Bolivia, spread rapidly among
399 human dwellings in the Southern Cone region of South America before its near eradication
400 in the 1990s[10]. Cytogenetic analyses suggest this early expansion was accompanied by a
401 substantial reduction in genome size[53], but the adaptive significance such a change is not

clear. The advantage of the *R. ecuadoriensis* system we describe is that it captures multiple parallel adaptive processes and; therefore, can assist in the identification of common evolutionary features associated with colonisation of the domestic environment. Despite limited genomic coverage, and with no *R. ecuadoriensis* reference genome available, we mapped outlier loci to genes in the *R. prolixus* draft genome, and found they are related to salivary enzyme production[41], as well as embryonic development[39]. Although these genes may have a role in domestic adaptation in triatomines, genome-wide association studies or quantitative trait locus mapping approaches are necessary to fully reveal the genomic architecture of adaptation to the domestic setting. Nevertheless, these findings motivate us to investigate further putative genes involved in local adaptation to the domestic environment such as blood-feeding[54], sensory cues and host-seeking behaviour[25,55], as well as human blood detoxification[54,56]. Recent data from our group in Loja province shows that, without doubt, domestic *R. ecuadoriensis* feed extensively on human blood[57].

Our analyses identified a strong signal of genetic IBD among *R. ecuadoriensis* populations across our study area. Geographic partitioning at this scale is consistent with limited autonomous dispersal capabilities of triatomines which, are, in the main, poor fliers[58]. Wind-blown dispersal observed in smaller vector species is unlikely in triatomines[59]. Passive dispersal of triatomine vectors alongside the movements of their human hosts, which certainly underpins the successful dispersal of other domesticated vector species, is more likely (e.g., *Aedes spp.* [60,61]). Lower IBD observed among domestic than wild settings may be consistent with passive dispersal alongside humans. We observed a similar phenomenon among parasite isolates from the same region in a previous study[32]. Nonetheless, our formal

425 exploration of the landscape drivers of vector dispersal did not reveal an important effect of
426 roads, and it is not clear to what extent human dispersal of vectors takes place based on our
427 data alone.
428
429 According to our landscape genomic analysis, elevation surface is a key predictor of
430 connectivity/discontinuity among *R. ecuadoriensis* populations. Our machine learning (ML)
431 optimisation procedure provides objective parameterisation of altitude resistance values to
432 *R. ecuadoriensis* gene flow[62]. Based on our landscape model predictions we were able to
433 construct a electric current map (Figure 4c) to assist medical entomologists and policy
434 makers in understanding vector dispersal routes. Current vector control strategies in Loja
435 target a single civic administrative unit (neighbourhood or town) for any given insecticidal
436 intervention[28]. Our data and model suggest this approach may be effective for certain
437 communities (e.g., SF, CG, NT and YS, Figure 4). However, for highly connected hubs (e.g.
438 BM, GA, CQ, AZ), successful longer term triatomine control (e.g., insecticide spraying,
439 house improvement, window nets, etc.) will depend on simultaneous intervention in multiple
440 connected communities.
441
442 In Ecuador, as with many other endemic regions in Latin America, efforts to control Chagas
443 disease may be complicated in the long term by substantial wild populations of secondary
444 triatomine vectors[16]. As with many other vector borne diseases, there is also a strong case
445 for the use of integrated vector management (IVM) for Chagas disease, where
446 improvements to housing, education, community engagement, in addition to bed net use and
447 insecticide spraying are all likely to be necessary to achieve sustained control[28,63]. Our data

clearly indicate that triatomines do invade houses in Loja and low-lying valleys provide routes for vector dispersal between communities and cost-effective IVM must be underpinned by this understanding of vector population structure. Fortunately, genomic and analytical tools can now furnish much of the detail, although better genomic resources for secondary triatomine vector species are required to reveal the process of vector adaptation to the human host. Targeting secondary vector species must now be a priority for health authorities, as these now represent the most pernicious and persistent barrier to controlling residual Chagas disease transmission.

Methods.

Sample collection and study area.

Rhodnius ecuadoriensis triatomine bugs (Supplementary Table 1) were derived from a larger collection in the Center for Research on Health in Latin America (CISeAL) of Pontificia Universidad Católica del Ecuador (PUCE). *Rhodnius prolixus* samples (n=6) were provided by the London School of Hygiene and Tropical Medicine and sequenced as an outgroup, as well as to assist with the decontamination of the of 2b-RAD reads and their mapping to functional regions in the draft *R. prolixus* genome[24]. *R. ecuadoriensis* individuals were collected using the one-hour-man method during field surveys across Loja, Ecuador from 2004 to 2018[28]. The triatomines were collected under Ecuadorian collection permits: N° 002–07 IC-FAU-DNBAPVS/MA; N° 003–2011-IC-FAU-DLP-MA; N° 006-IC-FAU-DLP-MA-2010; N° 010-IC-FAN-DPEO-MAE; N° 011–2015- IC-INF-VS-DPL-MA; MAE-DNB-CM-2015-0030

and internal mobilization guide N° 001-2018-UPN-VS-DPAL-MAE and N° 017-2018-UPN-VS-DPAL-MAE, All these samples were exported to the University of Glasgow by the scientific export authorization N°70-2018-EXP-CM-FAU-DNB/MA.

A widespread spatial sampling (Supplementary Figures 8, 9 and 10) of ecotopes (e.g., domestic and wild), altitudes (up to 1542.9 m.a.s.l.), vegetation types (e.g., tree/bush forest, cropland, etc.) and sites adjacent to different road infrastructure (e.g., highways, tertiary roads, etc.) was carried out in the study area.

Genomic DNA extraction and sequencing.

Genomic DNA (gDNA) was extracted in 88.2% (502/443) of the samples using a SSNT/Salt precipitation method[64] previously applied in triatomine bugs[65]. For each sample, gDNA concentration was > 25 ng/uL and 288.4 ng/UL (sd. ± 241.8) on average with purity ratios (260/280 and 260/230) of 1.87 (sd. ± 0.10) and 2.30 (sd. ± 0.97), respectively. gDNA was digested with the CspCI Type IIB restriction enzyme (IIB-REase - New England BioLabs, Inc.) which has shown to yield a high marker density in triatomine[65]. DNA fragments (36bp) were ligated to Illumina single-end adaptors and a specific barcode added during PCR amplification to construct 382 150bp 2bRAD libraries[66]. Libraries were homogenised to an approximate similar concentration, purified with magnetic beads[67] and pooled in two separate batches (n = 191). Each batch was sequenced separately on 1-flowcell (2 lanes) HiSeq 2500 (Illumina) Rapid Mode platform with a single-end (1x50 bp) setup using v2 SBS

chemistry at the Science for Life Laboratory (SciLifeLab, Stockholm, Sweden), which also implemented the reads demultiplexing and their in-house quality-filtering.

Bioinformatics of 2b-RAD sequenced data.

Data cleaning and decontamination. Demultiplexed raw data quality scores were verified in FastQC software v0.11.9 (http://www.bioinformatics.babraham.ac.uk/projects/fastqc/). 2.3% (16/689) Million reads (Mreads) were removed due to incomplete CspCI restriction site (36 bp) and having across read quality score below 30[68]. The 624.7 high quality Mreads with integrate restriction site had their Illumina adaptors and barcodes trimmed, and reads were forwarded (5'-3') using custom scripts. To exclude non-target sequences (Supplementary Methods 1.1), 1.2 Mreads (0.2%) reads mapping to bacteria, virus, archaeal, *Trypanosoma cruzi*[69] and *homo sapiens* (Genome Reference Consortium human build 38) genomes were removed using DeconSeq standalone v4.3[70] with an alignment identity threshold of 85% and Kraken[71] taxonomic classifier (Supplementary Figure 1). After decontamination, each sample yield on average 1.6 Million reads (interquartile range = 1.9 Mreads).

Optimisation and genotyping. As advised in refs.[72,73], we optimised (Supplementary Methods 1.1) STACKS v2.55[74] DENOVO_MAP.PL programme by varying at a time one of the main controlling parameters (-m, -M and -n; Supplementary Table 2) on each run while keeping the rest of the parameters at the setting used in early experiments (e.g., -m 5, -M 2, -n 1, -N 4, -alpha 0.01, -bound_low 0, -bound_high 0.01, -r 0.8, -min_maf 0.01[65]). The parameter combination yielding the highest number of SNPs with the least missing data and

516 genotyping error rate was chosen to be the optimal set. Genotypes below a quality score of
517 30, and samples with above 50% missing genotypes across sites and among loci were
518 removed from downstream analysis using the VCFtools software suite v0.1.5 5[75]. The
519 remaining missing genotypes (< 0.5%) were imputed using the k-nearest neighbour
520 genotype imputation (LDkNNi) method[76] implemented in the TASSEL software v5[77].
521
522 **Genomic differentiation between domestic and wild ecotopes**
523
524 **Genetic diversity and linkage disequilibrium.** Genetic diversity measures (e.g., observed
525 (H_O) and expected heterozygosity (H_E), inbreeding coefficient (F_{IS}) and percentage of loci in
526 Hardy-Weinberg equilibrium (% HWE)) were calculated for each collection site, and
527 ecotopes (domestic and wild) within collection sites, in the HIERFSTAT[78] and pegas[79]
528 packages in R[80]. Sample-size corrected Allelic richness (Ar) was calculated using the
529 rarefaction method[38] implemented in the PopGenReport[81] R package. To evaluate the
530 percentage of SNP markers in linkage disequilibrium (LD), correlation coefficient (r^2)
531 estimates were calculated between markers pairs using using the GUS-LD R package[82]
532 which revealed a very low percentage (< 0.20%). To observe whether genetic diversity
533 difference between ecotope pairs was significant, a permutation-based (10,000
534 permutations) two sample t-test was performed on each pair diversity values using the
535 RVAideMemoire R package (https://www.rdocumentation.org/packages/RVAideMemoire).
536
537 **Individual-based genomic differentiation.** Genomic differentiation among *R.*
538 *ecuadoriensis* domestic and wild samples within a subset of seven collection sites was

visualised in a neighbour-joining midpoint tree[83] (Figure 1b) built from Euclidean genetic distances of allele frequencies with the ape[84] R package. Tree components were edited in FigTree software v1.4.3 (http://tree.bio.ed.ac.uk/software/figtree/) to better illustrate domestic and wild samples and their overall clustering pattern. To explore samples genomic differentiation further, a DAPC[85] was performed in the same seven collection sites with the adegenet[86] R package (Figure 1c). The most likely *a priori* number of clusters was chosen based on the lowest Bayesian information criterion (BIC). In the DAPC, all principal components (PCs) and the eigenvectors of the first three DA discriminant functions were kept for visualizing the samples individual coordinates of different PCs linear combinations (Supplementary Figure 5).

Pairwise F_{ST} comparisons. To support previous hierarchical analyses, pairwise F_{ST} comparisons[43] were performed between *R. ecuadoriensis* from domestic and wild ecotopes within the seven collection sites (Figure 3b). In this study, F_{ST} was exploited as a measure of genomic connectivity (flow) between ecotopes within given collection sites. Specifically, Nei's F_{ST}[87] pairwise comparisons were computed in adegenet R package and tested at 5% significance via 999 permutations of individuals selected randomly within and between groups. P-values were corrected for multiple comparisons using the false discovery rate (FDR) method[88] in the function p.adjust of the stats R package[80].

Hierarchical F-statistics. *R. ecuadoriensis* molecular variation was explored at a four-level (e.g., among collection sites, among ecotopes (domestic or wild) within collection sites, among collection year within collection sites and among individuals within populations)

562 hierarchy of population structure. For each hierarchy, a F-statistic (with 95% C.I.) was
563 calculated, and its significance tested via 999 randomised permutations with the
564 HIERFSTAT R package. For comparison and given not all sites had both ecotopes, two
565 hierarchical analysis were performed, one with the total collection sites (n = 25) and the
566 other with a subset of collection sites (n = 7) with samples collected in both ecotopes
567 (Supplementary Table 4).
568
569 **Domestic-wild SNP association analyses.**
570
571 As a response of *R. ecuadoriensis* ecotopes fluxes in multiple collection sites across Loja,
572 we screened for SNP RADseq markers under a strong signal of selection (outlier loci). The
573 power for detecting outlier loci of four different approaches, Random Forest (RF) machine
574 learning (ML) classification algorithm (implemented in refs.[89–91]), redundancy analysis (RDA)
575 constraint ordination[92], and OutFlank[93] and fsthet[94] F_{ST}-outlier methods, was evaluated using
576 a roughly similar number of domestic (n= 56) and wild (n= 52) *R. ecuadoriensis* across Loja
577 province sharing a total of 2552 SNPs.
578
579 **Random Forest.** The RF algorithm[95] implemented in the randomForest[96] R package was
580 used to build a series of recursive decision trees, or forest, to classify domestic and wild *R.*
581 *ecuadoriensis* based on their shared SNPs (predictors) covarying to a specific ecotope
582 (response variable) (Supplementary Figure 6). Within each RF run, decision trees were
583 trained by random subsampling with replacement 66.6% of triatomine samples (training
584 dataset), for which aleatory selected SNPs were top-ranked classifiers when minimizing the

most within-ecotope variation (that is, partitioning triatomine by ecotope). Trained trees predictive power was tested with the remaining 33.3% triatomine samples ('Out-of-bag' test dataset) in which ecotope misclassification of samples estimated an OOB-ER for that RF run; SNPs importance classification accuracy was averaged among the total number of trees created in a given RF. Three independent (spatial structure-corrected) RFs with 100,000 trees were run and their convergence on SNPs importance classification accuracy was evaluated by Pearson's correlation test. Top-ranked SNPs (Figure 2a inset) among the three RFs (that is, importance classification accuracy above 3) were chosen for backwards purging, as implemented in refs.[90,97]. Backwards purging (Figure 2a) iteratively runs RFs starting with the full top-ranked SNPs and discarding the least important ones before the next iteration until only two were left. The subset with the lowest OOB-ER contained SNPs outlying strongly for the ecotope response.

Redundancy analysis. Outlier loci likely under selection were also identified using RDA multivariate constrained ordination[98] implemented in the vegan[99,100] R package. First, a matrix fitted values (Supplementary Figure 7a) were obtained using multivariate linear regression between a matrix of genotypes (response) and ecotopes (explanatory) with an additional term controlling for spatial structure (based on the three first axes of an individual principal coordinates of each sample). Then, principal component analysis (PCA) on the fitted values matrix resulted in a constrained axis composed from the variation explained, 'redundancy', by our explanatory variable (Supplementary Figure 7b). Overall RDA model and variation explained by the constrained RDA axis were tested for significance via 999 permutations designed for constrained correspondence analysis. Additionally, SNPs

608 coordinates were scaled and plotted in the ordination space to see their relationship with the
609 constraint axis, ecotope (Supplementary Figure 7c and Figure 2b). SNPs z-transformed
610 loadings (Supplementary Figure 7d) separated by ±2 and ±3 standard deviations
611 (permissible and conservative thresholds, respectively) from the mean distribution of the
612 total SNPs loadings in our RDA axis were considered under selection (Figure 2b) (for further
613 details on RDA see refs.[92,101,102]).
614
615 **F_{ST}-Heterozygosity outlier method.** The F_{ST}-Heterozygosity outlier method aims to identify
616 loci with strong allele differences among ecotopes. First, ecotope differentiation for each
617 locus is calculated using Wright's F_{ST} without sample correction. The distribution of these
618 values is expected to have a chi-squared shape. The main goal is inferring a null F_{ST}
619 distribution from neutral loci not strongly affected by diversifying selection[93]. Therefore, a
620 best-fit to the chi-squared F_{ST} distribution was achieved by trimming the lowest and highest
621 F_{ST} values (loci in the tails of the distribution are likely to be under effective diversifying
622 selection) and considering only the values in the centre (neutral loci and loci experiencing
623 spatial uniform balancing selection). Loci with unusual F_{ST} values relative to this fitted
624 distribution can be thought of experiencing additional diversifying selection[93,94]. We used two
625 R packages to accomplish this analysis, OutFlank[93] and fsthet[94], and compared the results
626 (Figure 2d). The difference between the packages is that fsthet uses smoothed quantiles of
627 the empirical F_{ST}-Heterozygosity distribution to identify outlier loci and does not assume a
628 particular distribution or model of evolution as compared to OutFlank. We set OutFlank
629 function with proportion of lower and upper loci trimmed to 0.06 and 0.35, respectively, and
630 the rest of the values to default.

631

632 **Mapping SNP outlier loci.** In order to identify genes that may be responsible for local
633 adaptation in the Chagas disease vector, *R. ecuadoriensis*, to the domestic environment we
634 mapped the SNPs found in the association analyses to the *R. prolixus* annotated genome[24].
635 We used the BWA alignment tool implemented in DeconSeq software v0.4.3[70] to map SNPs
636 sequences (38 bp) at a minimum alignment threshold of 85. The sequences of the regions
637 (60-300kb) in which our SNPs aligned were BLAST searched and compared to the *R.*
638 *prolixus* genome.

639

640 **Estimating gene flow with distance.** Matrices of genetic (F_{ST}[87]) and geographic (Km)
641 distances between the 25 collection sites, and between domestic and wild collection sites
642 separately, were obtained with the adegenet and raster[103] R packages, respectively. Mantel
643 tests[104] were performed on those matrices using the ecodist[105] R packages. Genetic and
644 geographic correlation between domestic and wild ecotopes was also viewed separately by
645 fitting a generalised least square (GLS) model with a maximum likelihood population effects
646 correction (MLPE)[106] implemented in the corMLPE (https://github.com/nspope/corMLPE/) R
647 package and assuming a linear relationship

648

649 $$Y_{ij} = \alpha + \beta(X_{ij} - \bar{x}) + H_i + \tau_{ij} + e_{ij} \qquad (\mathbf{eqn1})$$

650

651 between two distance matrices based on genetic and geographic distance measures, Y and
652 X, respectively. Centring the X_{ij} in about its mean, $\bar{x}$, removes the correlation between the

estimates of α and β[106]. H, determines the ecotope and the τ_{ij} term adds the MLPE random effect correlation structure.

Estimating gene flow with resistance.

Genetic distances. Given genomic differentiation between domestic and wild ecotopes was low, we combined all samples within a collection site and used collection site as the unit in our landscape genetic analysis. Collection site units are logistically and budgetary important when carrying out triatomine surveys and insecticide spraying. Using a landscape genomics mixed modelling framework (Supplementary Figure 2), we aimed to disentangle the effects of landscape heterogeneity on *R. ecuadoriensis* population structure and gene flow. A Hedrick's G_{ST} [42], which corrects for sampling limited populations[107], distance matrix among the 25 collection sites was obtained in the GenoDive v3.04[108] software. In addition, we ran a Pearson's correlation test between the Hedrick's G_{ST} matrix, and Meriman's standardised F_{ST}[44] and F_{ST}[43] matrices, calculated in the same software, to evaluate the consistency of genomic differentiation pattern among collection sites with different genetic distance measures.

GIS data collection and preparation. Three landscape variables (elevation, land cover and road network - hereafter, surfaces) were hypothesized to influence *R. ecuadoriensis* dispersal and gene flow (Supplementary Figures 8, 9 and 10). For the continuous surfaces (elevation surface), only monomolecular transformations (e.g., Supplementary Figure 12ab) with any possible shape and maximum parameters were explored to assume a linear

relationship in which gene flow decreases as altitude increases as hypothesised in other triatomine species[109]. Our categorical surfaces, land cover and road network, were reclassified as follows. Highly fragmented land cover categories (e.g., cultivated and managed areas) produced the least resistance to gene flow, whereas regular flooded areas and water bodies were barriers. Habitat fragmentation and human agricultural activities has been shown to affect triatomine populations dynamics[110]. Human-mediated passive triatomine dispersal has been suggested elsewhere[11], and therefore, we assumed roads would connect humans populations, and likely triatomines by passive carriage. High transitable roads (e.g., highways and tertiary roads) had the least resistant values, whereas absence of roads was a strong barrier (see Supplementary Table 9 & Supplementary Table 10). Original GIS surfaces were obtained from multiple sources (Supplementary Table 6) and transformed to have the same format (raster), resolution (250 m^2 grid), extent (~ 97 Km^2) and coordinate reference system (Universal Transverse Mercator (UTM)).

Spearman's rank correlation coefficient (rho) tests were run (Supplementary Table 8) and plotted (Supplementary Figure 11) on each pair of surfaces to ensure variables were uncorrelated (rho < 0.29 based on Cohen[111]). All three surfaces original values were transformed to the same scale (i.e., a minimum value of 1 and a maximum of 100) to meet our initial hypothesis.

ResistanceGA principle. The genetic algorithm[112] implemented in the R package, ResistanceGA[45], was used for multiple and sinlge-surface optimization of resistance values to gene flow in the above surfaces (Supplementary Figure 3). Briefly, ResistanceGA method is a powerful, flexible, stochastic and assumption-free framework based on an evolutionary

ML process that finds unbiased optimal resistance parameters (resistance weights values for a given surface) in space that best fits the genomic structure pattern[113]. The method works by correlating genomic (response) and effective (predictor) distances (derived from a random-walk commute time algorithm[114] – Supplementary Figure 4b) matrices through a maximum likelihood population effects[106] model and, on each iteration, evaluates the best resistance parameters based on a ML objective function, log-likelihood in our case. Simulating the process of evolution on each iteration, the best model and parameters are selected and pass over the next generation with some random change on parameter values to explore the parameter space widely.

Multiple surface optimisation. We performed three replicate runs to optimise all possible combinations of our surfaces (hereafter, composite surfaces), including surfaces individually (hereafter, single surfaces) to generate models with optimised resistance values. The major GA algorithm options were set to default, except for the 'pop.mult' which was set to 20 to increase the number of parameters to evaluate on each surface every iteration. All optimisation processes were run in parallel with 10-20 cores in a Debian cluster (http://userweb.eng.gla.ac.uk/umer.ijaz/#orion) at the University of Glasgow. Running times varied from days to weeks depending on surface size and number combined at a time.

Model selection. Composite and single surface models, including an intercept- only (null model) and a geographic distance (resistance grid cells are set to 1 to model isolation-by-distance) model were evaluated (Table 1) and the best model was selected based on the lowest AIC_c, AIC_c weight and Delta AIC_c. To confirm the robustness of the optimisation

722 surfaces and controlling for potential bias due to uneven distribution of sample locations in
723 the landscape, we carried out bootstrap resampling (10,000 iterations) in 85% of our sample
724 locations and then fit the subset to each of the effective distance matrices from the optimised
725 surfaces. After the bootstrapping analysis, the average AIC_c among all iterations and the
726 percentage a model was top over all iterations was used as a criterion to rank the best
727 model (Table 2).
728
729 **Landscape connectivity model.** We used the best optimised single (elevation surface)
730 resistance surface models to estimate landscape connectivity through a circuit theory
731 algorithm[46,47] (Supplementary Figure 4) implemented in the software CIRCUITSCAPE v5[115].
732 Here, our resistance surfaces were converted into electric networks (Supplementary Figure
733 4c) in which each grid cell represented a node connected to their neighbours by resistors of
734 different weight. Resistor weights were calculated from the average resistance values (i.e.,
735 optimised resistance values) of the two grid cells being connected. The algorithm applies a
736 simulated electric current between all pairs of focal nodes (collection sites) in the network to
737 estimate effective distances between them. A current density map (Figure 4c) was obtained
738 from those resistance distance estimations representing a random walk probability of
739 movement through our study area.
740
741 ## Data availability
742 Raw sequenced data will be uploaded to the Sequence Read Archive (SRA) repository on
743 publication.
744

Meterials & Correspondance

Correspondance to Martin Llewellyn and Luis Enrique Hernandez Castro

Code availability

Code for population, assosiation and landscape genomics analyses will be available via Github repository (github.com/lehernandezc/recuadoriensis) on publication.

References

1. Powell, J. R. & Tabachnick, W. J. History of domestication and spread of *Aedes aegypti*--a review. *Memórias do Instituto Oswaldo Cruz* vol. 108 11–17 (2013).
2. McBride, C. S. *et al.* Evolution of mosquito preference for humans linked to an odorant receptor. *Nature* **515**, 222–227 (2014).
3. Leftwich, P. T., Bolton, M. & Chapman, T. Evolutionary biology and genetic techniques for insect control. *Evolutionary Applications* vol. 9 212–230 (2016).
4. Powell, J. R. An Evolutionary Perspective on Vector-Borne Diseases. *Front. Genet.* **10**, 1266 (2019).
5. Manel, S. & Holderegger, R. Ten years of landscape genetics. *Trends Ecol. Evol.* **28**, 614–621 (2013).
6. Vreysen, M. J. B. *et al.* Sterile Insects to Enhance Agricultural Development: The Case of Sustainable Tsetse Eradication on Unguja Island, Zanzibar, Using an Area-Wide Integrated Pest Management Approach. *PLoS Negl. Trop. Dis.* **8**, e2857 (2014).
7. Schwabl, P. *et al.* Prediction and Prevention of Parasitic Diseases Using a Landscape Genomics Framework. *Trends Parasitol.* (2016) doi:10.1016/j.pt.2016.10.008.
8. Hemming-Schroeder, E., Lo, E., Salazar, C., Puente, S. & Yan, G. Landscape Genetics: A Toolbox for Studying Vector-Borne Diseases. *Front. Ecol. Evol.* **6**, 21 (2018).
9. WHO. WHO Chagas disease (American trypanosomiasis). https://www.who.int/news-room/fact-sheets/detail/chagas-disease-(american-trypanosomiasis) (2021).
10. Schofield, C. J. & Dias, J. C. The Southern Cone Initiative against Chagas disease. *Adv. Parasitol.* **42**, 1–27 (1999).

776 11. Hashimoto, K. & Schofield, C. J. Elimination of *Rhodnius prolixus* in Central America.
777 *Parasit. Vectors* **5**, 45 (2012).

778 12. Ceballos, L. A. *et al.* Hidden Sylvatic Foci of the Main Vector of Chagas Disease
779 *Triatoma infestans*: Threats to the Vector Elimination Campaign? *PLoS Negl. Trop.*
780 *Dis.* **5**, e1365 (2011).

781 13. Fitzpatrick, S., Feliciangeli, M. D., Sanchez-Martin, M. J., Monteiro, F. A. & Miles, M.
782 A. Molecular genetics reveal that silvatic *Rhodnius prolixus* do colonise rural houses.
783 *PLoS Negl. Trop. Dis.* **2**, e210 (2008).

784 14. Rodríguez-Planes, L. I., Gaspe, M. S., Enriquez, G. F. & Gürtler, R. E. Habitat-
785 Specific Occupancy and a Metapopulation Model of *Triatoma sordida* (Hemiptera:
786 Reduviidae), a Secondary Vector of Chagas Disease, in Northeastern Argentina. *J.*
787 *Med. Entomol.* **55**, 370–381 (2018).

788 15. Cantillo-Barraza, O., Chaverra, D., Marcet, P., Arboleda-Sánchez, S. & Triana-
789 Chávez, O. *Trypanosoma cruzi* transmission in a Colombian Caribbean region
790 suggests that secondary vectors play an important epidemiological role. *Parasites and*
791 *Vectors* **7**, (2014).

792 16. Grijalva, M. J., Villacís, A. G., Ocãa-Mayorga, S., Yumiseva, C. A. & Baus, E. G.
793 Limitations of selective deltamethrin application for triatomine control in central coastal
794 Ecuador. *Parasites and Vectors* **4**, 20 (2011).

795 17. Villacís, A. G. *et al.* Would tropical climatic variations impact the genetic variability of
796 triatomines: *Rhodnius ecuadoriensis*, principal vector of Chagas disease in Ecuador?
797 *Acta Trop.* **209**, 105530 (2020).

798 18. Brown, J. E. *et al.* Worldwide patterns of genetic differentiation imply multiple
799 'domestications' of *Aedes aegypti* , a major vector of human diseases. *Proc. R. Soc. B*
800 *Biol. Sci.* **278**, 2446–2454 (2011).

801 19. Powell, J. R., Gloria-Soria, A. & Kotsakiozi, P. Recent history of *Aedes aegypti*: Vector
802 genomics and epidemiology records. *BioScience* vol. 68 854–860 (2018).

803 20. Soria-Carrasco, V. *et al.* Stick insect genomes reveal natural selection's role in
804 parallel speciation. *Science (80-.).* **344**, 738–742 (2014).

805 21. Zumaya-Estrada, F. A. *et al.* North American import? Charting the origins of an
806 enigmatic Trypanosoma cruzi domestic genotype. *Parasites and Vectors* **5**, 226
807 (2012).

808 22. Piccinali, R. V. *et al.* Molecular Population Genetics and Phylogeography of the
809 Chagas Disease Vector *Triatoma infestans* in South America. *J. Med. Entomol.* **46**,
810 796–809 (2009).

811 23. Frantz, L. A. F. *et al.* Ancient pigs reveal a near-complete genomic turnover following
812 their introduction to Europe. *Proc. Natl. Acad. Sci. U. S. A.* **116**, 17231–17238 (2019).

813 24. Mesquita, R. D. *et al.* Genome of *Rhodnius prolixus* , an insect vector of Chagas

disease, reveals unique adaptations to hematophagy and parasite infection. *Proc. Natl. Acad. Sci.* **112**, 14936–14941 (2015).

25. Marchant, A. *et al.* Under-Expression of Chemosensory Genes in Domiciliary Bugs of the Chagas Disease Vector *Triatoma brasiliensis*. *PLoS Negl. Trop. Dis.* **10**, (2016).

26. Liu, Q. *et al.* A chromosomal-level genome assembly for the insect vector for Chagas disease, *Triatoma rubrofasciata*. *Gigascience* **8**, (2019).

27. Tigano, A. & Friesen, V. L. Genomics of local adaptation with gene flow. *Mol. Ecol.* **25**, 2144–2164 (2016).

28. Grijalva, M. J. *et al.* Comprehensive Survey of Domiciliary Triatomine Species Capable of Transmitting Chagas Disease in Southern Ecuador. *PLoS Negl. Trop. Dis.* **9**, e0004142 (2015).

29. Grijalva, M. J., Suarez-Davalos, V., Villacis, A. G., Ocaña-Mayorga, S. & Dangles, O. Ecological factors related to the widespread distribution of sylvatic *Rhodnius ecuadoriensis* populations in southern Ecuador. *Parasit. Vectors* **5**, 17 (2012).

30. Villacís, A. G., Grijalva, M. J. & Catalá, S. S. Phenotypic Variability of *Rhodnius ecuadoriensis* Populations at the Ecuadorian Central and Southern Andean Region. *J. Med. Entomol.* **47**, 1034–1043 (2010).

31. Villacís, A. G. *et al.* Pioneer study of population genetics of *Rhodnius ecuadoriensis* (Hemiptera: Reduviidae) from the central coastand southern Andean regions of Ecuador. *Infect. Genet. Evol.* **53**, 116–127 (2017).

32. Ocaña-Mayorga, S., Llewellyn, M. S., Costales, J. A., Miles, M. A. & Grijalva, M. J. Sex, Subdivision, and Domestic Dispersal of *Trypanosoma cruzi* Lineage I in Southern Ecuador. *PLoS Negl. Trop. Dis.* **4**, e915 (2010).

33. Costales, J. A. *et al. Trypanosoma cruzi* population dynamics in the Central Ecuadorian Coast. *Acta Trop.* (2015) doi:10.1016/j.actatropica.2015.07.017.

34. De Souza, R. D. C. M. *et al.* Population dynamics of *Triatoma vitticeps* (Stål, 1859) in Itanhomi, Minas Gerais, Brazil. *Mem. Inst. Oswaldo Cruz* **103**, 14–20 (2008).

35. Kamimura, E. H. *et al.* Drivers of molecular and morphometric variation in *Triatoma brasiliensis* (Hemiptera: Triatominae): The resolution of geometric morphometrics for populational structuring on a microgeographical scale. *Parasites and Vectors* **13**, 455 (2020).

36. Flores-Ferrer, A., Marcou, O., Waleckx, E., Dumonteil, E. & Gourbière, S. Evolutionary ecology of Chagas disease; what do we know and what do we need? *Evol. Appl.* **11**, 470–487 (2018).

37. Monteiro, F. A., Wesson, D. M., Dotson, E. M., Schofield, C. J. & Beard, C. B. Phylogeny and molecular taxonomy of the rhodniini derived from mitochondrial and nuclear DNA sequences. *Am. J. Trop. Med. Hyg.* **62**, 460–465 (2000).

851 38. El Mousadik, A. & Petit, R. J. High level of genetic differentiation for allelic richness
852 among populations of the argan tree [Argania spinosa (L.) Skeels] endemic to
853 Morocco. *Theor. Appl. Genet.* **92**, 832–839 (1996).

854 39. Lavore, A., Esponda-Behrens, N., Pagola, L. & Rivera-Pomar, R. The gap gene
855 Krüppel of *Rhodnius prolixus* is required for segmentation and for repression of the
856 homeotic gene sex comb-reduced. *Dev. Biol.* **387**, 121–129 (2014).

857 40. Lavore, A., Pagola, L., Esponda-Behrens, N. & Rivera-Pomar, R. The gap gene giant
858 of *Rhodnius prolixus* is maternally expressed and required for proper head and
859 abdomen formation. *Dev. Biol.* **361**, 147–155 (2012).

860 41. Ribeiro, J. M. . *et al.* Exploring the sialome of the blood-sucking bug *Rhodnius*
861 *prolixus*. *Insect Biochem. Mol. Biol.* **34**, 61–79 (2004).

862 42. Hedrick, P. W. A STANDARDIZED GENETIC DIFFERENTIATION MEASURE.
863 *Evolution (N. Y).* **59**, 1633–1638 (2005).

864 43. Weir, B. S. & Cockerham, C. C. ESTIMATING F -STATISTICS FOR THE ANALYSIS
865 OF POPULATION STRUCTURE. *Evolution (N. Y).* **38**, 1358–1370 (1984).

866 44. Meirmans, P. G. USING THE AMOVA FRAMEWORK TO ESTIMATE A
867 STANDARDIZED GENETIC DIFFERENTIATION MEASURE. *Evolution (N. Y).* **60**,
868 2399–2402 (2006).

869 45. Peterman, W. E. ResistanceGA□: An R package for the optimization of resistance
870 surfaces using genetic algorithms. *Methods Ecol. Evol.* **9**, 1638–1647 (2018).

871 46. McRae, B. H., Dickson, B. G., Keitt, T. H. & Shah, V. B. USING CIRCUIT THEORY
872 TO MODEL CONNECTIVITY IN ECOLOGY, EVOLUTION, AND CONSERVATION.
873 *Ecology* **89**, 2712–2724 (2008).

874 47. Kivimäki, I., Shimbo, M. & Saerens, M. Developments in the theory of randomized
875 shortest paths with a comparison of graph node distances. *Phys. A Stat. Mech. its*
876 *Appl.* **393**, 600–616 (2014).

877 48. Paucar, R., Moreno-Viguri, E. & Pérez-Silanes, S. Challenges in Chagas Disease
878 Drug Discovery: A Review. *Curr. Med. Chem.* **23**, 3154–3170 (2016).

879 49. Olivera, M. J. *et al.* Risk factors for treatment interruption and severe adverse effects
880 to benznidazole in adult patients with Chagas disease. *PLoS One* **12**, (2017).

881 50. Sosa-Estani, S. Advances and challenges in the treatment of Chagas disease - a
882 global perspective. *Int. J. Infect. Dis.* **73**, 51 (2018).

883 51. Kilpatrick, A. M. *et al.* Genetic Influences on Mosquito Feeding Behavior and the
884 Emergence of Zoonotic Pathogens. *Am J Trop Med Hyg* **77**, 667–671 (2007).

885 52. Gillies, M. T. Selection for host preference in *Anopheles gambiae*. *Nature* **203**, 852–
886 854 (1964).

887 53. Panzera, F. *et al.* Evolutionary and dispersal history of *Triatoma infestans*, main
888 vector of Chagas disease, by chromosomal markers. *Infect. Genet. Evol.* **27**, 105–113
889 (2014).

890 54. Santiago, P. B. *et al.* Proteases of haematophagous arthropod vectors are involved in
891 blood-feeding, yolk formation and immunity - a review. *Parasites and Vectors* vol. 10
892 1–20 (2017).

893 55. Guerenstein, P. G. & Lazzari, C. R. Host-seeking: How triatomines acquire and make
894 use of information to find blood. *Acta Trop.* **110**, 148–158 (2009).

895 56. Sterkel, M. *et al.* Tyrosine Detoxification Is an Essential Trait in the Life History of
896 Blood-Feeding Arthropods. *Curr. Biol.* **26**, 2188–2193 (2016).

897 57. Ocaña-Mayorga, S. *et al.* Triatomine feeding profiles and *Trypanosoma cruzi*
898 infection, implications in domestic and sylvatic transmission cycles in Ecuador.
899 *Pathogens* **10**, 1–17 (2021).

900 58. Vazquez-Prokopec, G. M., Ceballos, L. A., Kitron, U. & Gürtler, R. E. Active dispersal
901 of natural populations of *Triatoma infestans* (Hemiptera: Reduviidae) in rural
902 northwestern Argentina. *J. Med. Entomol.* **41**, 614–21 (2004).

903 59. Huestis, D. L. *et al.* Windborne long-distance migration of malaria mosquitoes in the
904 Sahel. *Nature* vol. 574 404–408 (2019).

905 60. Brown, J. E. *et al.* HUMAN IMPACTS HAVE SHAPED HISTORICAL AND RECENT
906 EVOLUTION IN *AEDES AEGYPTI* , THE DENGUE AND YELLOW FEVER
907 MOSQUITO. *Evolution (N. Y).* **68**, 514–525 (2014).

908 61. Medley, K. A., Jenkins, D. G. & Hoffman, E. A. Human-aided and natural dispersal
909 drive gene flow across the range of an invasive mosquito. *Mol. Ecol.* **24**, 284–295
910 (2015).

911 62. Peterman, W. E. *et al.* A comparison of popular approaches to optimize landscape
912 resistance surfaces. *Landsc. Ecol.* **34**, 2197–2208 (2019).

913 63. Castro-Arroyave, D., Monroy, M. C. & Irurita, M. I. Integrated vector control of Chagas
914 disease in Guatemala: a case of social innovation in health. *Infect. Dis. Poverty* **9**, 25
915 (2020).

916 64. Aljanabi, S. M. & Martinez, I. Universal and rapid salt-extraction of high quality
917 genomic DNA for PCR-based techniques. *Nucleic Acids Res.* **25**, 4692–4693 (1997).

918 65. Hernandez-Castro, L. E. *et al.* 2b-RAD genotyping for population genomic studies of
919 Chagas disease vectors: *Rhodnius ecuadoriensis* in Ecuador. *PLoS Negl. Trop. Dis.*
920 **11**, e0005710 (2017).

921 66. Wang, S., Meyer, E., McKay, J. K. & Matz, M. V. 2b-RAD: a simple and flexible
922 method for genome-wide genotyping. *Nat. Methods* **9**, 808–10 (2012).

923 67. DeAngelis, M. M., Wang, D. G. & Hawkins, T. L. Solid-phase reversible immobilization

for the isolation of PCR products. *Nucleic Acids Res.* **23**, 4742–3 (1995).

68. O'Leary, S. J., Puritz, J. B., Willis, S. C., Hollenbeck, C. M. & Portnoy, D. S. These aren't the loci you'e looking for: Principles of effective SNP filtering for molecular ecologists. *Mol. Ecol.* **27**, 3193–3206 (2018).

69. Franzén, O. *et al.* Shotgun Sequencing Analysis of *Trypanosoma cruzi* I Sylvio X10/1 and Comparison with T. cruzi VI CL Brener. *PLoS Negl. Trop. Dis.* **5**, e984 (2011).

70. Schmieder, R. & Edwards, R. Fast Identification and Removal of Sequence Contamination from Genomic and Metagenomic Datasets. *PLoS One* **6**, e17288 (2011).

71. Wood, D. E. & Salzberg, S. L. Kraken: ultrafast metagenomic sequence classification using exact alignments. *Genome Biol.* **15**, R46 (2014).

72. Mastretta-Yanes, A. *et al.* Restriction site-associated DNA sequencing, genotyping error estimation and de novo assembly optimization for population genetic inference. *Mol. Ecol. Resour.* **15**, 28–41 (2015).

73. Paris, J. R., Stevens, J. R. & Catchen, J. M. Lost in parameter space: a road map for stacks. *Methods Ecol. Evol.* **8**, 1360–1373 (2017).

74. Catchen, J., Hohenlohe, P. A., Bassham, S., Amores, A. & Cresko, W. A. Stacks: an analysis tool set for population genomics. *Mol. Ecol.* **22**, 3124–40 (2013).

75. Danecek, P. *et al.* The variant call format and VCFtools. *Bioinformatics* **27**, 2156–2158 (2011).

76. Money, D. *et al.* LinkImpute: Fast and Accurate Genotype Imputation for Nonmodel Organisms. *G3 (Bethesda).* **5**, 2383–90 (2015).

77. Bradbury, P. J. *et al.* TASSEL: software for association mapping of complex traits in diverse samples. *Bioinformatics* **23**, 2633–2635 (2007).

78. GOUDET, J. hierfstat, a package for r to compute and test hierarchical F-statistics. *Mol. Ecol. Notes* **5**, 184–186 (2005).

79. Paradis, E. pegas: an R package for population genetics with an integrated-modular approach. *Bioinformatics* **26**, 419–420 (2010).

80. R Development Core Team. R: A language and environment for statistical computing. (2016).

81. Adamack, A. T. & Gruber, B. PopGenReport: Simplifying basic population genetic analyses in R. *Methods Ecol. Evol.* **5**, 384–387 (2014).

82. Bilton, T. P. *et al.* Linkage disequilibrium estimation in low coverage high-throughput sequencing data. *Genetics* **209**, 389–400 (2018).

83. Saitou, N. & Nei, M. The neighbor-joining method: a new method for reconstructing phylogenetic trees. *Mol. Biol. Evol.* **4**, 406–425 (1987).

84. Paradis, E. & Schliep, K. ape 5.0: an environment for modern phylogenetics and evolutionary analyses in R. *Bioinformatics* **35**, 526–528 (2019).

85. Jombart, T., Devillard, S. & Balloux, F. Discriminant analysis of principal components: a new method for the analysis of genetically structured populations. *BMC Genet.* **11**, 94 (2010).

86. Jombart, T. adegenet: a R package for the multivariate analysis of genetic markers. *Bioinformatics* **24**, 1403–5 (2008).

87. Nei, M. Analysis of gene diversity in subdivided populations. *Proc. Natl. Acad. Sci. U. S. A.* **70**, (1973).

88. Benjamini, Y. & Hochberg, Y. Benjamini-1995.pdf. *Journal of the Royal Statistical Society B* vol. 57 289–300 (1995).

89. Brieuc, M. S. O., Ono, K., Drinan, D. P. & Naish, K. A. Integration of Random Forest with population-based outlier analyses provides insight on the genomic basis and evolution of run timing in Chinook salmon (*Oncorhynchus tshawytscha*). *Mol. Ecol.* **24**, 2729–2746 (2015).

90. Laporte, M. *et al.* RAD sequencing reveals within-generation polygenic selection in response to anthropogenic organic and metal contamination in North Atlantic Eels. *Mol. Ecol.* **25**, 219–237 (2016).

91. Brieuc, M. S. O., Waters, C. D., Drinan, D. P. & Naish, K. A. A practical introduction to Random Forest for genetic association studies in ecology and evolution. *Mol. Ecol. Resour.* **18**, 755–766 (2018).

92. Forester, B. R., Lasky, J. R., Wagner, H. H. & Urban, D. L. Comparing methods for detecting multilocus adaptation with multivariate genotype-environment associations. *Mol. Ecol.* **27**, 2215–2233 (2018).

93. Whitlock, M. C. & Lotterhos, K. E. Reliable detection of loci responsible for local adaptation: Inference of a null model through trimming the distribution of FST. *Am. Nat.* **186**, S24–S36 (2015).

94. Flanagan, S. P. & Jones, A. G. Constraints on the FST–Heterozygosity Outlier Approach. *J. Hered.* **108**, 561–573 (2017).

95. Breiman, L. Random Forests. *Mach. Learn.* **45**, 5–32 (2001).

96. Liaw, A. & Weiner, M. Classification and Regression by randomForest. *R news 2(3)* 18–22 https://www.r-project.org/doc/Rnews/Rnews_2002-3.pdf (2002).

97. Holliday, J. A., Wang, T. & Aitken, S. Predicting Adaptive Phenotypes From Multilocus Genotypes in Sitka Spruce (*Picea sitchensis)* Using Random Forest. (2012) doi:10.1534/g3.112.002733.

98. Legendre, P. & Legendre, L. Canonical analysis. in *Developments in Environmental Modelling* vol. 24 625–710 (2012).

997 99. Oksanen, J. *Multivariate Analysis of Ecological Communities in R: vegan tutorial*.
998 http://cc.oulu.fi/~jarioksa/opetus/metodi/vegantutor.pdf (2015).

999 100. Oksanen, J. *et al.* vegan: Community Ecology Package. (2019).

1000 101. Forester, B. R., Jones, M. R., Joost, S., Landguth, E. L. & Lasky, J. R. Detecting
1001 spatial genetic signatures of local adaptation in heterogeneous landscapes. *Mol. Ecol.*
1002 **25**, 104–120 (2016).

1003 102. Capblancq, T., Luu, K., Blum, M. G. B. & Bazin, E. Evaluation of redundancy analysis
1004 to identify signatures of local adaptation. *Mol. Ecol. Resour.* **18**, 1223–1233 (2018).

1005 103. Hijmans, R. J. & Van Etten, J. raster: Geographic analysis and modeling with raster
1006 data. (2012).

1007 104. Mantel, N. The Detection of Disease Clustering and a Generalized Regression
1008 Approach. *Cancer Res.* **27**, 209–220 (1967).

1009 105. Goslee, S. C. & Urban, D. L. The ecodist Package for Dissimilarity-based Analysis of
1010 Ecological Data. *J. Stat. Softw.* **22**, 1–19 (2007).

1011 106. Clarke, R. T., Rothery, P. & Raybould, A. F. Confidence limits for regression
1012 relationships between distance matrices: Estimating gene flow with distance. *J. Agric.*
1013 *Biol. Environ. Stat.* **7**, 361–372 (2002).

1014 107. MEIRMANS, P. G. & HEDRICK, P. W. Assessing population structure: FST and
1015 related measures. *Mol. Ecol. Resour.* **11**, 5–18 (2011).

1016 108. MEIRMANS, P. G. & VAN TIENDEREN, P. H. genotype and genodive: two programs
1017 for the analysis of genetic diversity of asexual organisms. *Mol. Ecol. Notes* **4**, 792–
1018 794 (2004).

1019 109. Parra-Henao, G., Suárez-Escudero, L. C. & González-Caro, S. Potential Distribution
1020 of Chagas Disease Vectors (Hemiptera, Reduviidae, Triatominae) in Colombia, Based
1021 on Ecological Niche Modeling. *J. Trop. Med.* **2016**, (2016).

1022 110. Grijalva, M. J., Terán, D. & Dangles, O. Dynamics of sylvatic chagas disease vectors
1023 in coastal Ecuador is driven by changes in land cover. *PLoS Negl. Trop. Dis.* **8**, e2960
1024 (2014).

1025 111. Cohen, J. A power primer. *Psychol. Bull.* **112**, 155–159 (1992).

1026 112. Scrucca, L. GA: A package for genetic algorithms in R. *J. Stat. Softw.* **53**, 1–37
1027 (2013).

1028 113. Peterman, W. E. *et al.* A comparison of popular approaches to optimize landscape
1029 resistance surfaces. *Landsc. Ecol.* 1–12 (2019) doi:10.1007/s10980-019-00870-3.

1030 114. Fouss, F., Pirotte, A., Renders, J. M. & Saerens, M. Random-walk computation of
1031 similarities between nodes of a graph with application to collaborative
1032 recommendation. *IEEE Trans. Knowl. Data Eng.* **19**, 355–369 (2007).

115. Shah, V. B. & Mcrae, B. Circuitscape: A Tool for Landscape Ecology. in *Proceedings of the 7th Python in Science Conference (SciPy 2008)* (eds. Varoquaux, G., Vaught, T. & Millman, J.) 62–66 (2008).

Acknowledgements

We thank P. Johnson for advice in statistical analyses, W. Peterman for helpful advice on ResistanceGA analysis, the entomological team at CISeAL for sample collection and M. Babbucci for proving custom scripts for 2b-RAD raw data cleaning. This work was possible thanks to the Mexican Council of Science and Technology doctorate scholarship (CVU Number 613766) awarded to L.E.H.C., the National Institutes of Health (NIH) grant number R15 AI105749-01A1 allocated to MJG who is PI, as well as RCUK Engagment Network (EP/T003782/1) which supported co-author interactions. Funding was also received from Pontifical Catholic University of Ecuador to MJG (grant # C13025, E13027, E13037, H13174, I13048). ELL was supported by the National Institute of General Medical Sciences of the NIH, United States (Award Numbers P20GM130418). The funders had no role in study design, data collection and analysis, decision to publish, or preparation of the manuscript.

Author contributions

L.E.H.C., M.S.L., and M.J.G. designed the study. L.E.H.C. and M.S.L. wrote the manuscript with contributions from M.J.G., J.A.C., and E.L.L. A.G.V., A.J., B.C., C.C.D., S.O.M., C.A.Y., A.B., B.A., L.M., E.L.L. revised and edited the manuscript. A.G.V., S.O.M., C.A.Y., and J.A.C. collected and provided triatomine samples from Loja Ecuador. L.E.H.C performed DNA extraction and 2b-RAD library preparation. B.A. performed NGS Illumina HiSeq. L.E.H.C analysed the data with contributions from A.J. in the association analysis, B.C. in data decontamination/bioinformatics, C.C.D., and E.L.L in the landscape genomic analyses.

Competing interests

The authors declare no competing interests.

Supplementary information

Supplementary Table 1 (excel file)

Supplementary Methods (docx file)

Figures 1 - 4

Figures in the order of appearance in main text.

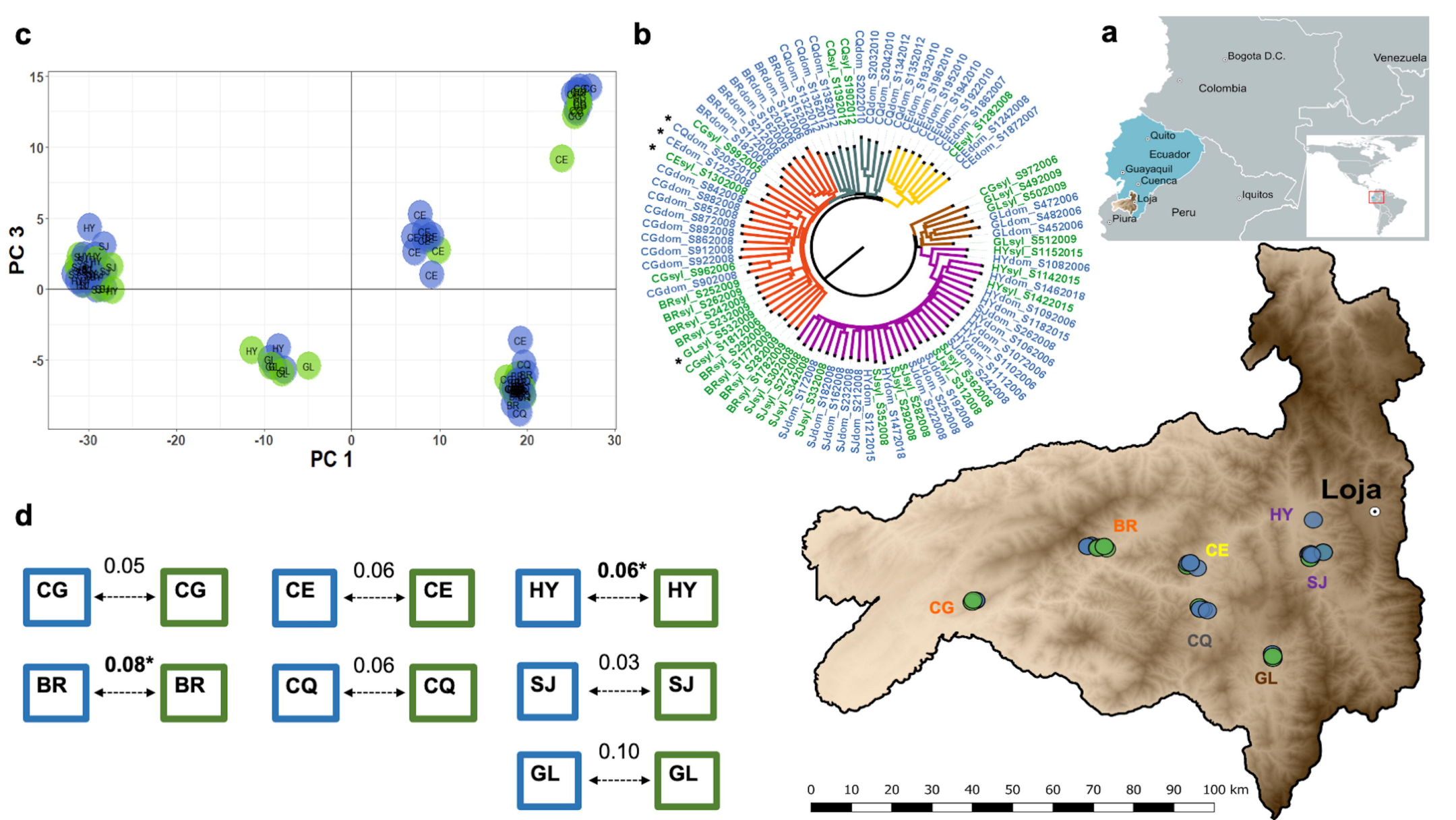
c
PC 3
PC 1
15
10
5
0
-5
-30
-20
-10
0
10
20
30
HY
SJ
CE
GL
CQ
BR
b
a
Bogota D.C.
Venezuela
Colombia
Quito
Ecuador
Guayaquil
Cuenca
Loja
Iquitos
Piura
Peru
Loja
BR
HY
CE
SJ
CG
CQ
GL
0
10
20
30
40
50
60
70
80
90
100 km
d
CG
0.05
CG
CE
0.06
CE
HY
0.06*
HY
BR
0.08*
BR
CQ
0.06
CQ
SJ
0.03
SJ
GL
0.10
GL

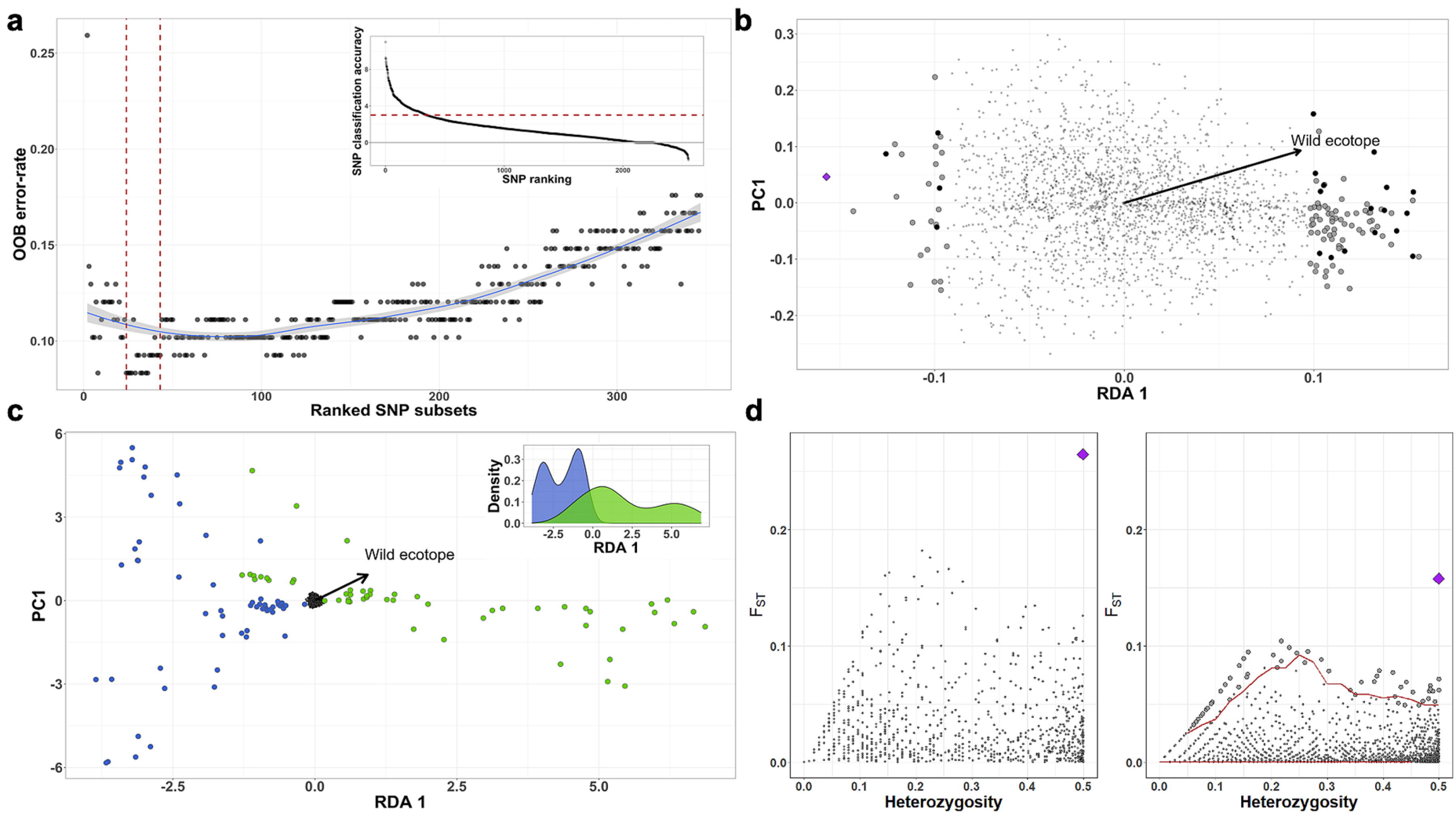
a
OOB error-rate
Ranked SNP subsets
SNP classification accuracy
SNP ranking
b
PC1
RDA 1
Wild ecotope
c
PC1
RDA 1
Wild ecotope
Density
d
F_{ST}
Heterozygosity
F_{ST}
Heterozygosity

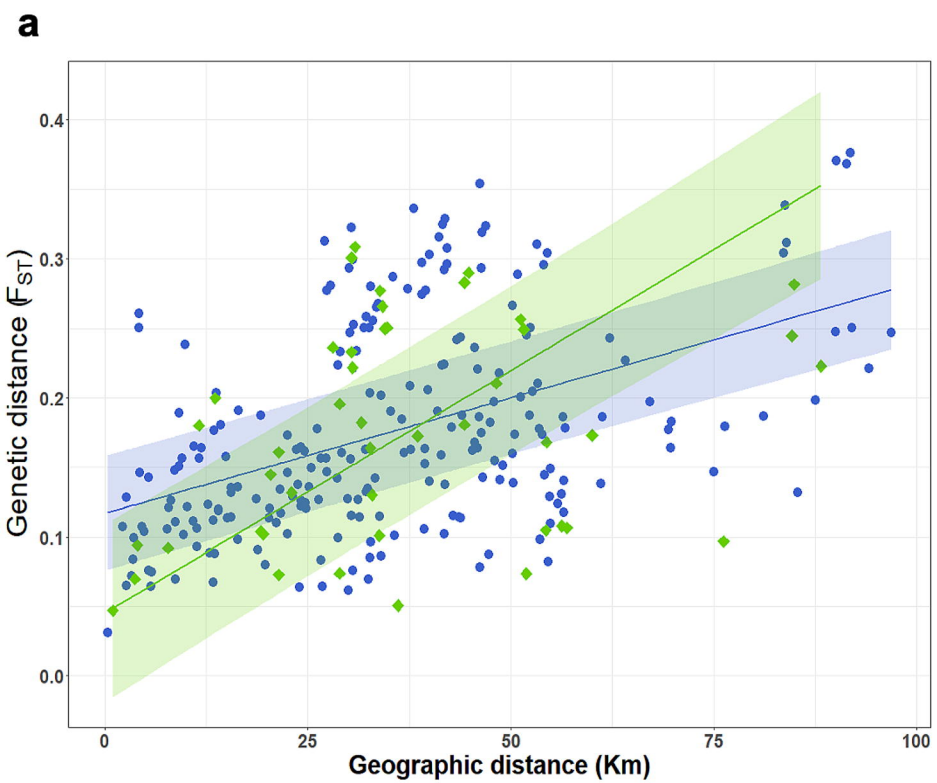
a
Genetic distance (F_{ST})
0.4
0.3
0.2
0.1
0.0
0
25
50
75
100
Geographic distance (Km)

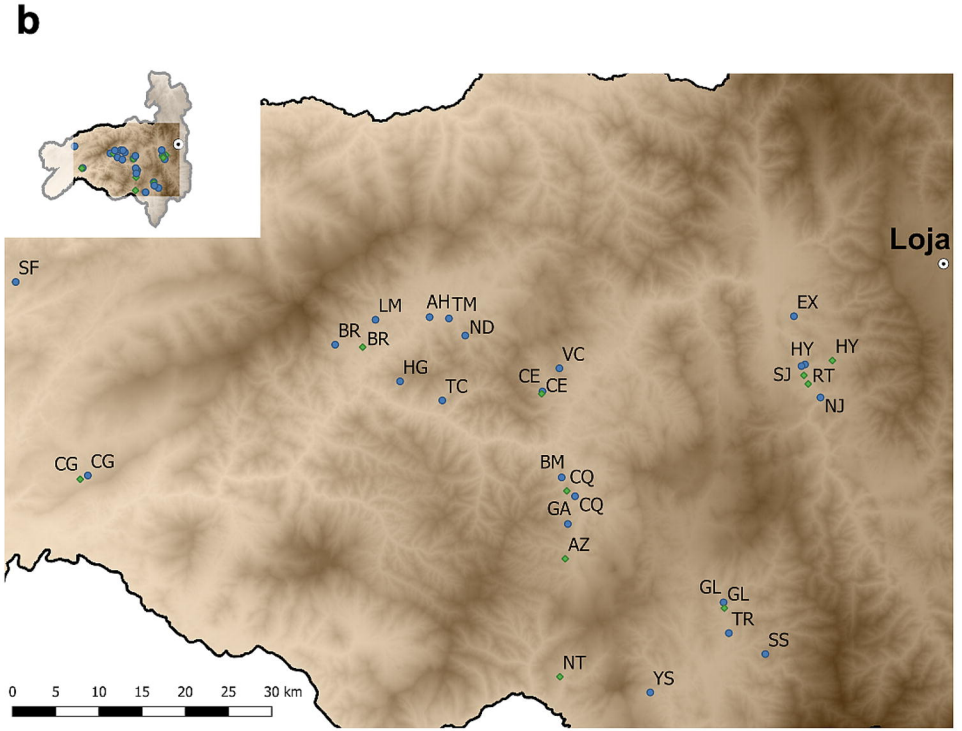
b
Loja
SF
LM
AH
TM
ND
BR
BR
HG
TC
VC
CE
CE
EX
HY
HY
SJ
RT
NJ
CG
CG
BM
CQ
GA
CQ
AZ
GL
GL
TR
SS
NT
YS
0
5
10
15
20
25
30 km

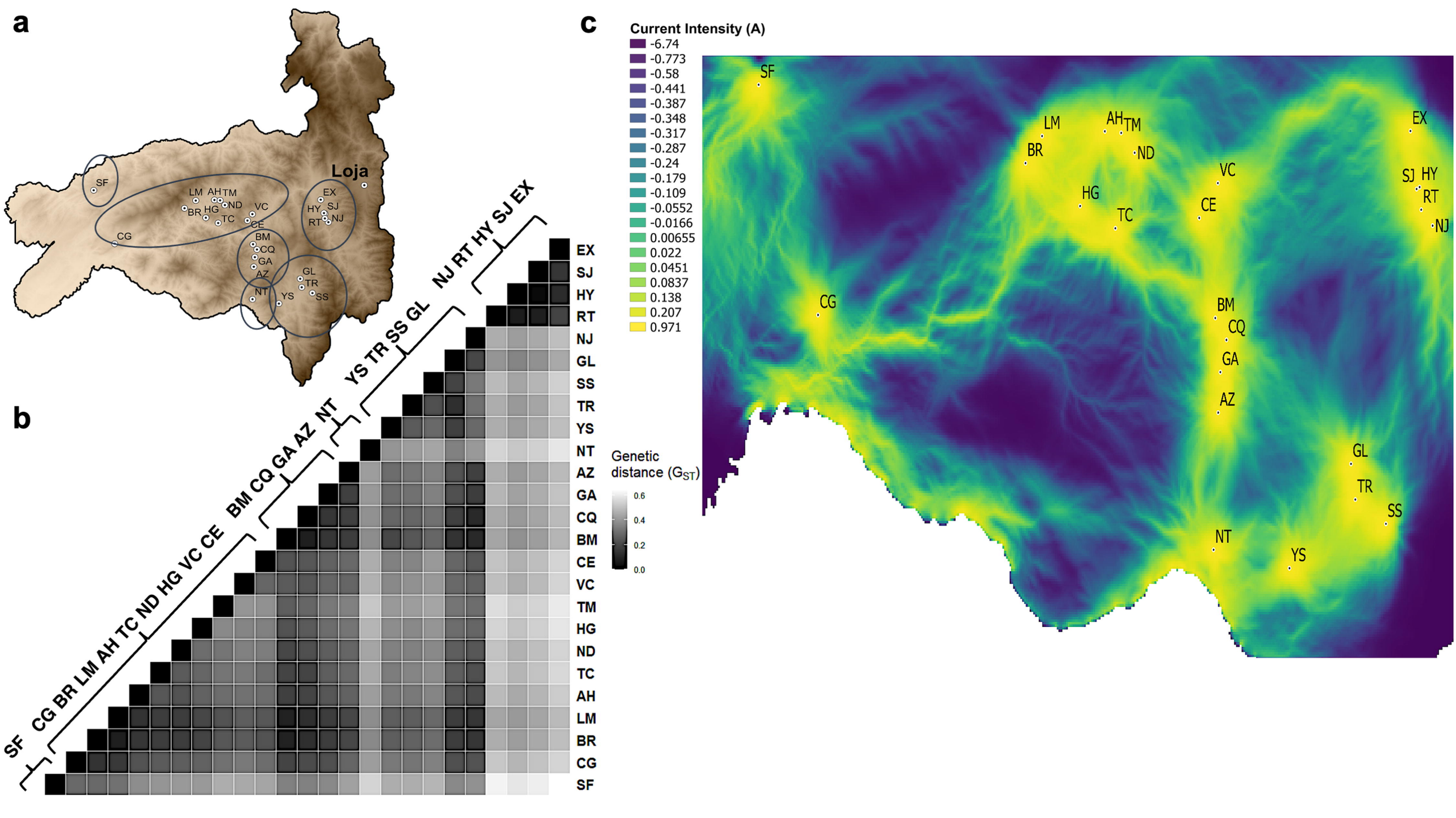
a
Loja
SF
LM AH TM
BR HG ND VC
TC CE
CG
EX
HY SJ
RT NJ
BM
CQ
GA
AZ
NT
YS
GL
TR
SS
b
SF CG BR LM AH TC ND HG VC CE BM CQ GA AZ NT YS TR SS GL NJ RT HY SJ EX
EX SJ HY RT NJ GL SS TR YS NT AZ GA CQ BM CE VC TM HG ND TC AH LM BR CG SF
c
Current Intensity (A)
-6.74
-0.773
-0.58
-0.441
-0.387
-0.348
-0.317
-0.287
-0.24
-0.179
-0.109
-0.0552
-0.0166
0.00655
0.022
0.0451
0.0837
0.138
0.207
0.971
Genetic distance (G_{ST})
0.6
0.4
0.2
0.0
SF
LM
AH TM
BR
ND
EX
SJ HY
RT
NJ
VC
HG
TC
CE
CG
BM
CQ
GA
AZ
GL
TR
SS
NT
YS